



## Original article

## 2,4,5-Trisubstituted thiazole derivatives: A novel and potent class of non-nucleoside inhibitors of wild type and mutant HIV-1 reverse transcriptase



Zhongliang Xu <sup>a,1</sup>, Mingyu Ba <sup>b,1</sup>, Hua Zhou <sup>a</sup>, Yingli Cao <sup>b</sup>, Chaojun Tang <sup>a</sup>, Ying Yang <sup>b</sup>, Ricai He <sup>a</sup>, Yu Liang <sup>a</sup>, Xuemei Zhang <sup>b</sup>, Zhenzhong Li <sup>a</sup>, Lihong Zhu <sup>a</sup>, Ying Guo <sup>b,\*</sup>, Changbin Guo <sup>a,\*</sup>

<sup>a</sup> Department of Chemistry, Capital Normal University, Beijing 100048, China

<sup>b</sup> State Key Laboratory of Bioactive Substance and Function of Natural Medicines, Institute of Materia Medica, Chinese Academy of Medical Sciences and Peking Union Medical College, Beijing 100050, China

## ARTICLE INFO

## Article history:

Received 24 April 2014

Received in revised form

18 July 2014

Accepted 21 July 2014

Available online 22 July 2014

## Keywords:

HIV-1

Non-nucleoside reverse transcriptase inhibitors

2,4,5-Trisubstituted thiazole derivatives

Molecular modeling

Three-dimensional quantitative structure activity relationship

## ABSTRACT

Novel 2,4,5-trisubstituted thiazole derivatives (TSTs) were designed and synthesized as HIV-1 non-nucleoside reverse transcriptase inhibitors (NNRTIs). Among the thirty-eight synthesized target compounds, thirty TSTs showed potent inhibition against HIV-1 replication in wild type HIV-1 at sub-micromolar concentrations (from 0.046 to 9.59  $\mu\text{M}$ ). Compounds **21**, **23** and **24** were also tested on seven NNRTI-resistant HIV-1 strains, and all exhibited inhibitory effects with fold changes in  $\text{IC}_{50}$  ranging from 2.6 to 111, which were better than those of nevirapine (15.6-fold–371-fold). Docking simulations of compound **24** revealed a reasonable mechanism for the binding mode, and three-dimensional quantitative structure activity relationship (3-DQSAR) studies on this novel series of TST further elucidated the structure–activity relationship (SAR). The results suggested the great potential of TSTs as a novel class of NNRTIs with antiviral efficacy and a good resistance profile.

© 2014 Elsevier Masson SAS. All rights reserved.

## 1. Introduction

Three decades have passed since the human immunodeficiency virus (HIV) was identified as the causative agent of acquired immunodeficiency syndrome (AIDS) [1,2]. It has been estimated that 35.3 (32.2–38.8) million people were living with HIV globally at the end of 2012 [3]. Highly active antiretroviral therapy (HAART), a combination of three to four drugs, has significantly decreased the morbidity and mortality rates of HIV patients [4,5]. However, drug resistance and severe drug–drug interactions limit the clinical efficacy of HAART [6–8], thus, the search for novel anti-HIV drugs continues.

Non-nucleoside reverse transcriptase inhibitors (NNRTIs) play a very important role in HAART. Currently, five NNRTI drugs have been approved by the U.S. FDA for AIDS therapy, including three first-generation drugs (nevirapine (NVP), delavirdine, and efavirenz (EFZ)) and two second-generation drugs (etravirine and rilpivirine) [9,10]. Despite the advantages of high potency and low toxicity, rapid viral drug resistance to first-generation NNRTI drugs has limited their clinical use. The most prominent mutants selected by first-generation NNRTI therapy are the K103N and the Y181C variants [11,12]. Consequently, addressing drug resistance is the focus of current NNRTI research and development, and the emergence of resistance to these drugs led us to search for new NNRTIs with a higher genetic barrier against clinically relevant mutant strains [13].

Unbiased compound screening for HIV-1 replication inhibitors led to the discovery of a novel structural class of NNRTIs, 2,4,5-trisubstituted thiazole derivatives (TSTs). Compound **2** and **3** blocked HIV-1 replication with  $\text{IC}_{50}$  values of 2.3  $\mu\text{M}$  and 4.4  $\mu\text{M}$ , respectively [14]. However, compound **1** showed no anti-HIV activity at 10  $\mu\text{M}$ . Compound **4** was synthesized with a benzyl group

Abbreviations list: TSTs, 2,4,5-trisubstituted thiazole derivatives; DMSO, dimethyl sulfoxide; VSVG, vesicular stomatitis virus glycoprotein.

\* Corresponding authors.

E-mail addresses: [yingguo6@imm.ac.cn](mailto:yingguo6@imm.ac.cn) (Y. Guo), [guocb@cnu.edu.cn](mailto:guocb@cnu.edu.cn) (C. Guo).

<sup>1</sup> Authors Zhongliang Xu and Mingyu Ba contributed equally.

in place of the dialkyl group in compounds **1–3**, and the  $IC_{50}$  decreased to 0.65  $\mu M$ . This result encouraged us to perform further structure–activity relationship (SAR) studies of this series of compounds. Until now, there have been no reports of thiazoles as a scaffold for HIV NNRTIs. In the present article, we used **4** as the lead compound for the design and synthesis with the following strategies: (i) the use of different substituents at positions 2 and 4 of the thiazole ring; (ii) modification with different linkers between the thiazole ring and the phenyl ring at position 2; and (iii) the introduction of substituents at position 5 of the thiazole. The anti-HIV replication activity was evaluated for all target compounds, and the most potent derivatives were also tested for activity against NNRTI-resistant strains (Fig. 1).

## 2. Results and discussion

The synthesis of compounds **42a–42m** and **38** is shown in Scheme 1. Appropriate acetophenones and benzaldehydes were condensed to give chalcones, which were then hydrogenated, brominated, and condensed with an appropriate sulfur source to give 2-aminothiazoles. The intermediate 2-aminothiazoles could also be elaborated using various methods, after which the 2-aminothiazoles were condensed with appropriate benzaldehydes to afford the Schiff bases. Reduction of the Schiff bases afforded most of the target compounds. Compounds **27** and **31** were obtained through chemical transformations similar to those in Scheme 1 with the use of different starting materials. Compounds **1**, **2**, **37** were obtained through coupling of **43** with various substituted amines. Compound **35** was obtained by methylation of compound **7** and compound **3** was obtained through demethylation of compound **2** (Scheme 2).

Because this series of compounds possesses a new structural scaffold, we attempted rational of the compounds to explore the SAR. Simple replacement of the *N,N*-dimethyl group of **1** with the *N,N*-diethyl group of **2** and the benzyl group of **4** led to a significant increase in the activity. We speculated that a hydrophobic group in this location might increase the activity. The optimization of lead compound **4** initially focused on the substituent of the phenyl ring at position 2 of the thiazole ring, and this phenyl ring was replaced with different aromatic rings. The structures and the activities are shown in Table 1. Comparison of compounds **5** (6.97  $\mu M$ ), **6** (0.82  $\mu M$ ) and **7** (0.31  $\mu M$ ), compounds **11** (0.80  $\mu M$ ) and **12** (1.47  $\mu M$ ) shows that para-substituents are superior to ortho- and meta-substituents. The activities of compounds **5** and **6**, where the ‘–OCH<sub>3</sub>’ is at the ortho- or meta-position, are reduced to 6.97  $\mu M$  and 0.82  $\mu M$ , respectively, compared with compound **7**. Similarly, the activity of compound **12**, with the introduction of ‘–NO<sub>2</sub>’ at the meta-position of the phenyl ring, decreased significantly compared to compound **11**, which has an ‘–NO<sub>2</sub>’ at the para-position. In addition, the activities of ortho-disubstituted compound **14** (7.21  $\mu M$ ), ortho- and meta-disubstituted compound **15** (5.20  $\mu M$ ) and 3,4,5-trisubstituted compound **17** are greatly decreased

compared with those of other compounds or disappear altogether. Interestingly, compound **16** (0.33  $\mu M$ ), which possesses an ‘–OH’ at the para-position of the phenyl ring in compound **6**, clearly shows higher activity than compounds **6** and **8**, which have a mono ‘–OH’ at the para-position. We speculate that this increase may occur because the ‘–OCH<sub>3</sub>’ at the meta-position and the ‘–OH’ at the para-position participate in an intramolecular hydrogen bond, thus forming a 5-membered hydrogen-bonded ring, which generates unknown changes in the recognition site. These changes require further investigation (Fig. 2).

In contrast, by placing different substituents at the para-position on the phenyl ring to observe the changes in activity, we found no causal relationships between the electronic properties of the substituents and the activities. Replacing the ‘–OCH<sub>3</sub>’ on position 4 of compound **7** with the more potent electron-donating *N,N*-dimethyl group resulted in a decrease in the activity of compound **9**. Additionally, replacing the same ‘–OCH<sub>3</sub>’ with the electron-withdrawing groups ‘–F’ or ‘–NO<sub>2</sub>’ also decreased the activities of compounds **10** and **11**.

Finally, replacing the phenyl ring at position 2 of the thiazole ring with 2-furanyl, 3-pyridyl or 2-naphthyl, we obtained compounds **18**, **19**, and **20**. Compared with compound **4**, compounds **18** (1.00  $\mu M$ ), **19** (4.67  $\mu M$ ), and **20** (0.96  $\mu M$ ) are less active by varying degrees. Of these three compounds, the activity of compound **19**, with a 3-pyridyl substituent, shows the greatest decrease to 4.67  $\mu M$ . This result further illustrates that meta-substitution is unfavorable to activity. However, the activity of compound **20**, with a 2-naphthyl ring, shows the smallest decrease. Combining these observations with the hypothesis that compound **16** may form a 5-membered ring through a hydrogen bond between ‘–OCH<sub>3</sub>’ and ‘–OH’, we surmise that an appropriate increase of the bulk of the aromatic ring in this location may be beneficial for the activity. However, this hypothesis requires further research (Fig. 2).

Table 2 presents the structures and activities of compounds **21–28**. In compounds **21–28**, we changed the substitution at the 4 position of the thiazole ring while retaining the structure at positions 2 and 5 of compound **7**, which showed the highest inhibition activity in Table 1. The results show that changing the substituents at position 4 has a huge impact on the activity of the compounds. Of these results, the activities of compounds **21**, **23**, and **24** are equivalent to those of **NVP**, and the activities increased ten-fold compared with lead compound **4**. Removing the *p*-methoxy from the phenyl ring at position 4 of compound **7** afforded compound **28** and increased the inhibition activity to 0.18  $\mu M$ . In contrast, the activity of compound **22** (1.21  $\mu M$ ), which is mono *p*-substituted, declined substantially compared with that of compound **28**, suggesting that mono substitution at the para-position is not preferred. However, the activity of compound **23**, in which another ‘–F’ has been introduced at the ortho-position of compound **22**, increased substantially to 0.064  $\mu M$ , suggesting that this substitution is preferred. According to these results, compounds **24** and **25**, which have 2-Cl and 2,4-Cl<sub>2</sub> substituents on the phenyl ring at position 4,

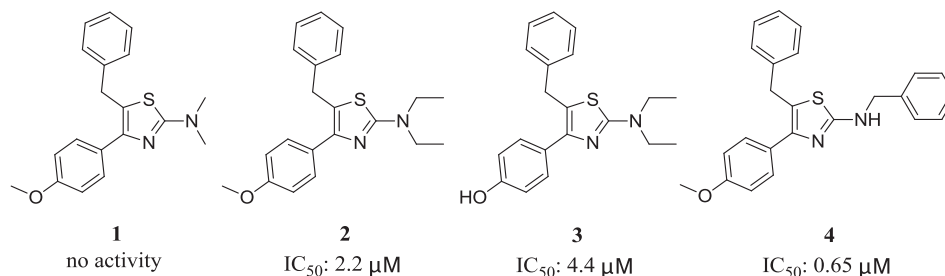
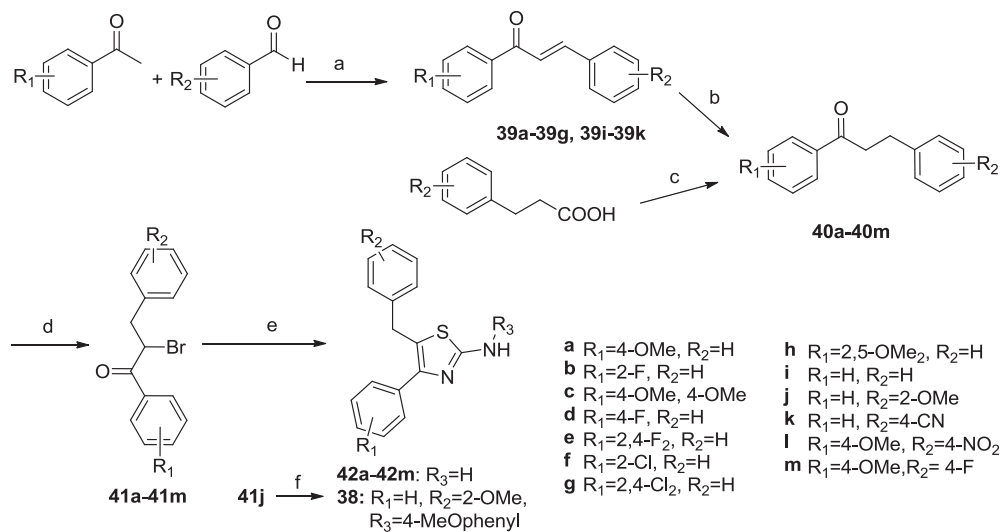
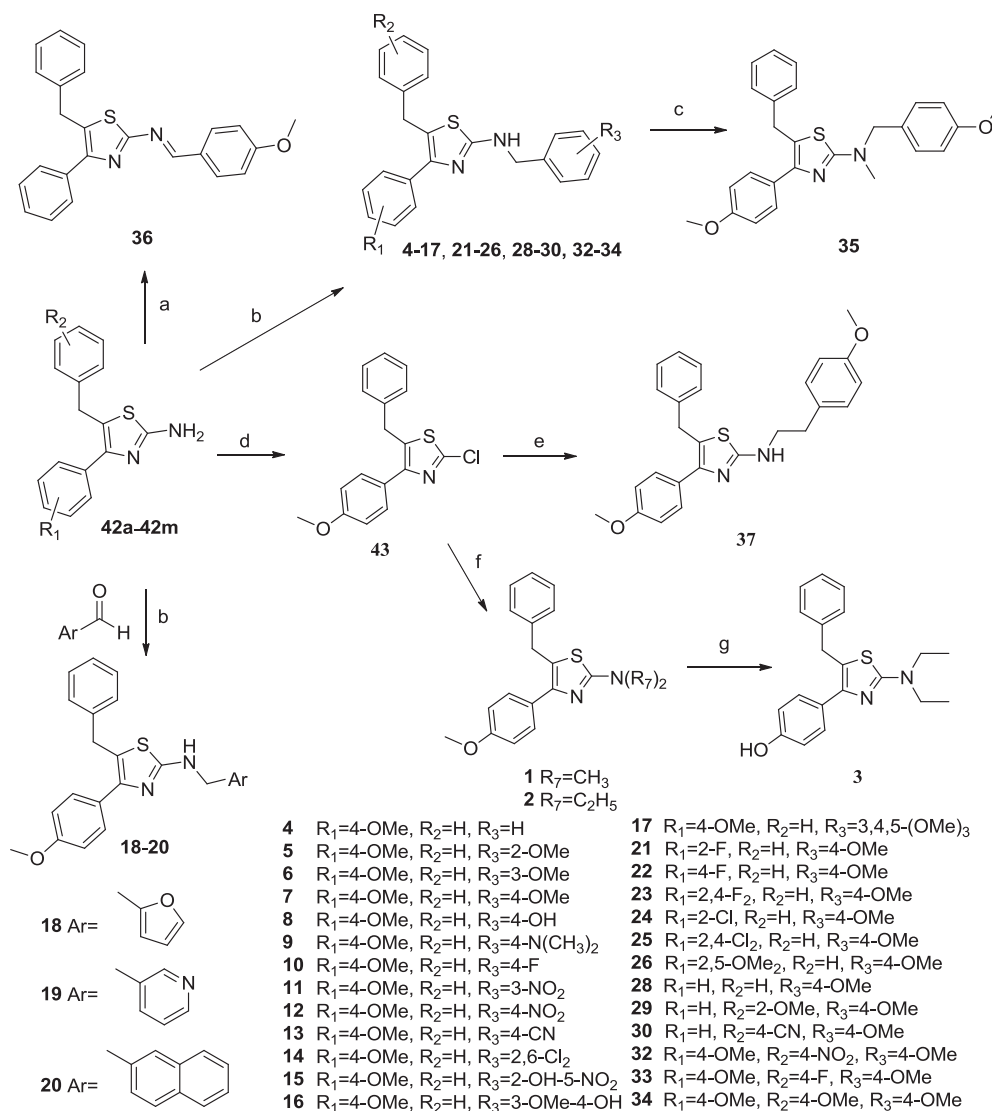


Fig. 1. Structures and activities of **1**, **2**, **3**, and **4**.



**Scheme 1.** Synthesis of **42a–42m** and **38**. Reagents and conditions: (a) 10% NaOH, EtOH, rt, 5–10 h, 70–90%; (b)  $H_2$ , Pd/C, EA, rt, 3–4 h, 80–95%; (c) i)  $SOCl_2$ , reflux; ii) substituted benzene,  $CH_2Cl_2$ ,  $AlCl_3$ ; (d)  $Br_2$ ,  $AlCl_3$ ,  $CHCl_3$ , 0 °C, 5–10 h; (e) thiourea (**42a–42m**)/*N*-(4-methoxyphenyl) thiourea (**38**),  $CH_3COONa$ , EtOH, 80 °C, 10–15 h, 70–80%.



**Scheme 2.** Synthesis of **1–26**, **28–30**, and **32–37**. Reagents and conditions: (a) 4-methoxybenzaldehyde, *p*-toluenesulfonic acid, toluene, 130 °C, 10–24 h; (b) i) substituted benzaldehyde, *p*-toluenesulfonic acid, toluene, 130 °C, 10–24 h, ii)  $NaBH_4$ , EtOH, rt, 2–5 h, 50–85%; (c) DMF, NaH, MeI, 40 °C, 2–5 h, 68%; (d) isopentyl nitrite,  $CuCl_2$ ,  $CH_3CN$ ; 30%; (e) 4-methoxyphenethylamine,  $LiOH \cdot H_2O$ , KI, DMF/ $H_2O$ , 50%; (f)  $LiOH \cdot H_2O$ , DMF or diethylamine/ $H_2O$ ; (g)  $BBr_3$ ,  $CHCl_2$ , 63.2%.

**Table 1**  
Chemical structures and cell-based antiviral assay of compounds **4–20**<sup>a</sup> against WT HIV-1.

Compd	R <sub>1</sub>	IC <sub>50</sub> <sup>b</sup> (μM)
4		0.65
5		6.97
6		0.82
7		0.31
8		0.64
9		0.87
10		0.66
11		0.80
12		1.47
13		0.45
14		7.21
15		5.20
16		0.33
17		>10
18		1.00
19		4.67

**Table 1** (continued)

Compd	R <sub>1</sub>	IC <sub>50</sub> <sup>b</sup> (μM)
<b>20</b>		0.96
<b>NVP</b>	—	0.031
<b>EFV</b>	—	0.00084

<sup>a</sup> All tested compounds had no cytotoxicity at a final concentration of 10 μM.

<sup>b</sup> Inhibitory concentration 50% (IC<sub>50</sub>, μM) was calculated from the dose–infectivity curves.

respectively, were synthesized. As expected, compound **24** showed high activity at 0.046 μM, whereas the activity of compound **25** decreased to 0.14 μM. Thus, we hypothesize that halogen substituents at the ortho-position may be most favorable for activity, whereas the contribution of para-substitution to the activity is small. Compound **26** has a 2,5-dimethoxy substitution pattern on the phenyl ring at position 4, and its activity decreased to 6.20 μM, suggesting that this substitution substantially negatively affected the inhibition. In compound **27**, the phenyl ring at position 4 was replaced with a furan-2-yl, which didn't improve the inhibition compared with compound **28**.

Based on the results from the first two rounds of optimization, we explored the effects of substituents at position 5 of the thiazole ring on the activity, and the results are shown in Table 3. Removing the phenyl ring from this position and methyl substitution resulted in a significant loss of inhibition against HIV replication (compound **31**), showing the necessity of an aromatic ring in the 5 position. Compared to compound **28**, the introduction of an '–OCH<sub>3</sub>' at the ortho-position of the phenyl ring significantly increased the activity of compound **29**, whereas introduction of a '–CN' in the para-position significantly reduced the activity of compound **30**. Moreover, compounds **32**, **33** and **34**, obtained by introducing '4-NO<sub>2</sub>', '4-F', and '4-OMe', respectively, to the phenyl ring at position 5 of the thiazole in compound **7**, completely lost inhibition activity against HIV-1 RT. These results indicate that the substituents on the phenyl ring have an important influence on activity; further research will more fully elucidate these effects.

The different linkers between the thiazole ring and the phenyl ring at position 2 may affect the conformation of the molecule in space, thus influencing its activity. Finally, we explored different linkers on the 2 positions of the thiazole ring as the Table 4 shows. In compound **35**, one 'H' on the amino group was replaced with a methyl group, but the activity did not change significantly compared with compound **7**, suggesting that H at this position may not be a hydrogen bond donor. Compound **36**, the Schiff base of compound **10**, showed no inhibition against HIV-1 replication, implying that limiting the rotation of the single bond of the carbon and nitrogen atoms may negatively impact the activities of the TSTs. Extending the linker on position 2 to three atoms resulted in the loss of inhibition for compound **37**. Shortening the linker to one

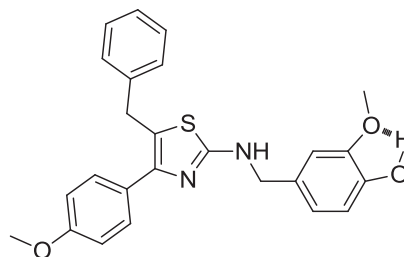
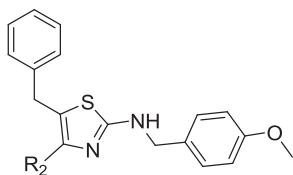


**Fig. 2.** The speculated 5-membered ring forming from a hydrogen bond between '–OCH<sub>3</sub>' and '–OH' of **16**.

**Table 2**  
Chemical structures and cell-based antiviral assay of compounds **21–28**<sup>a</sup> against WT HIV-1.



Compd	R <sub>2</sub>	IC <sub>50</sub> <sup>b</sup> (μM)
<b>21</b>		0.062
<b>22</b>		1.21
<b>23</b>		0.064
<b>24</b>		0.046
<b>25</b>		0.14
<b>26</b>		6.20
<b>27</b>		0.70
<b>28</b>		0.18
<b>NVP</b>	—	0.031
<b>EFV</b>	—	0.00084

<sup>a</sup> All tested compounds showed no cytotoxicity at a final concentration of 10 μM.

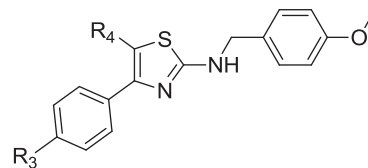
<sup>b</sup> Inhibitory concentration 50% (IC<sub>50</sub>, μM) was calculated from the dose–infectivity curves.

atom to connect the amino directly to the phenyl ring also resulted in the loss of inhibition for compound **38**. These findings implied that optimal inhibition requires a two-atom linker on position 2.

### 3. A brief summary of SAR

Fig. 3 shows a brief summary of the SAR of the TSTs. We divide the scaffold of the TSTs into five parts. In addition to the central thiazole ring, A, B, C, and D represent four structural segments: the side chain in the 2 position, the 4 and 5 substituents, and the linker on position 2 of the thiazole ring, respectively. In part A, compound **7** with a 4-methoxyphenyl showed the most potent inhibition against HIV-1. Retaining the structure from compound **7** at positions 2 and 5 and changing the substitution at the 4 position of the thiazole ring shows the SAR of part B; 2-fluorophenyl, 2,4-difluorophenyl and 2-chlorophenyl turned out to be the optimal substituents for B. Modifications on part C suggest that a phenyl ring is preferred. The most favorable length of the linker for activity is two atoms.

**Table 3**  
Chemical structures and cell-based antiviral assay of compounds **29–34**<sup>a</sup> against WT HIV-1.



Compd	R <sub>3</sub>	R <sub>4</sub>	IC <sub>50</sub> <sup>b</sup> (μM)
<b>29</b>	H		0.13
<b>30</b>	H		4.79
<b>31</b>	OMe	CH <sub>3</sub>	9.59
<b>32</b>	OMe		>10
<b>33</b>	OMe		>10
<b>34</b>	OMe		>10
<b>NVP</b>	—	—	0.031
<b>EFV</b>	—	—	0.00084

<sup>a</sup> All tested compounds showed no cytotoxicity at a final concentration of 10 μM.

<sup>b</sup> Inhibitory concentration 50% (IC<sub>50</sub>, μM) was calculated from the dose–infectivity curves.

### 4. Resistance

Time-of-drug addition assay was performed to identify the target of the active compounds. The results exhibited that the compounds' anti-HIV replication activity was due to the inhibition of viral reverse transcription process (Supplementary data). Since HIV drug resistance was the major cause of clinical treatment failure, five compounds, **8**, **9**, **21**, **23** and **24**, were selected for evaluation of their inhibition activities against NNRTI-resistant HIV-1 replication. Seven NNRTI-resistant HIV-1 recombinant virus models were used: HIV<sub>RT-Y181C</sub>, HIV<sub>RT-K103N</sub>, HIV<sub>RT-L100I/RT-K103N</sub>, HIV<sub>RT-Y188L</sub>, HIV<sub>RT-K103N/RT-P225H</sub>, HIV<sub>RT-K103N/RT-G190A</sub> and HIV<sub>RT-K103N/RT-V108I</sub>. The results in Table 5 indicated that compounds **21**, **23** and **24** showed good inhibition against replication of the most common drug-resistant strains. Compound **23** exhibited the most potent inhibitory activity against six of the seven resistant strains, with multiples of drug resistance ranging from 6.3 to 156, which are better than the positive control drug efavirenz, the latter fold-ranges from 5.4 to 2394.2.

### 5. Molecular modeling studies

Pursuing this line of research, we undertook docking and 3D-QSAR studies on a training set. Surflex-Dock was used to perform the docking study, and the comparative molecular field analysis (CoMFA) and the comparative molecular similarity index analysis (CoMSIA) methods were used to perform the 3D-QSAR study. The aim of this work was to establish reliable 3D-QSAR models and

**Table 4**  
Chemical structures and cell-based antiviral assay of compounds **35**–**38**<sup>a</sup> against WT HIV-1.

Compd	Structure	IC <sub>50</sub> <sup>b</sup> (μM)
35		0.37
36		>10
37		>10
38		>10
NVP		0.031
EFV		0.00084

<sup>a</sup> All tested compounds showed no cytotoxicity at a final concentration of 10 μM.

<sup>b</sup> Inhibitory concentration 50% (IC<sub>50</sub>, μM) was calculated from the dose–infectivity curves.

determine the most likely binding conformations for these compounds.

Compound **24**, which showed the highest activity against the WT HIV-1, was used as a representative to conduct the docking experiments in the WT HIV-1 RT non-nucleoside binding site (NNBS) and study the binding mode of the TSTs. To take into account the flexibility of the experimental NNBS, the structural data of six RTs (1c1b [15]; 1c1c [15]; 1ikx [16]; 2b5j [17]; 3lak [18]; 2rki [19]) were selected. The Surflex [20] program was used to dock **24** into all six RTs. In all cases, the docked conformations (either the first ranked or the most populated cluster representing conformations) agreed well with each other, and a nearly identical binding mode for **24** with all RTs was observed. The chemical

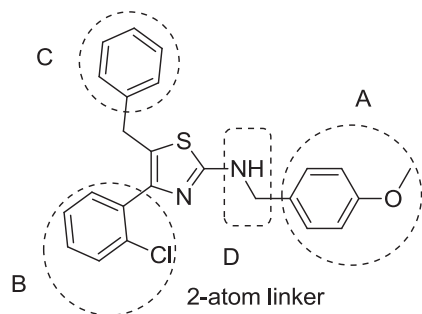


**Fig. 3.** SAR of the TSTs.

features of **24** shared a common binding mode in all RTs: (i) the nitrogen atom of the thiazole forms a hydrogen bond with the K103 amino group on the side chain; (ii) the side chain at the 2-position of the thiazole occupies a pocket formed mainly by the side chains of F227, P225, P236, and D237; (iii) the phenyl ring at the 5 position of the thiazole has a  $\pi$ – $\pi$  stacking interaction with Y181 or Y188 and fits in a small hydrophobic pocket composed of the side chains of Y181, Y188, and W229; (iv) the 2-chlorine atom of the phenyl at the 4 position of the thiazole possesses favorable contacts with G190 or K103, based on the distance between them (Fig. 4).

## 6. CoMFA/CoMSIA 3-DQSAR of TSTs

### 6.1. Training set

A training set of twenty-five TST derivatives was used to develop the 3-DQSAR. Compounds **2**, **4**, **6**, **21** and **26** were used as the test set, the rest were used as the training set.

### 6.2. Alignment rules

Alignment rules determine the ability of the CoMFA and CoMSIA models to predict and make general assumptions, as they determine the conformation and orientation of all molecules within the 3D lattice [21]. Because the best-docked geometries agreed with the crystallographic data of the complex for all compounds (and thus were already aligned), the receptor-based alignment rules were obtained from docking experiments of the training set in the NNBS extracted from the TT1/RT complex (PDB: 2rki); they were directly submitted to CoMFA and CoMSIA studies [22].

### 6.3. Definition of the 3D-QSAR models

CoMFA and CoMSIA were used to establish QSAR models. In CoMFA, the steric and electrostatic fields were calculated separately for each molecule using an sp<sup>3</sup> carbon as the probe atom with a charge of +1.00 (default probe atom in Sybyl) and energy cutoff values of 30 kcal/mol for both the steric and electrostatic fields [23]. The automatically generated CoMFA fields were scaled by the CoMFA-STD method in SYBYL. The partial least squares (PLS) method was used to linearly correlate the CoMFA fields to the inhibitory activity values [24–26]. A cross-validation analysis was performed using the leave-one-out (LOO) method, in which one compound is removed from the dataset, and its activity is predicted using the model derived from the rest of the dataset [27]. The final model was constructed to yield the highest q<sup>2</sup>, and the corresponding conventional correlation coefficient r<sup>2</sup>, its standard errors, and the F ratio were also calculated.

Table 6 shows the PLS statistics of the CoMFA and CoMSIA models. The two methods were employed to derive a 3D-QSAR model consisting of a training set of 25 ligands. The leave-one-out partial least-squares (PLS) analysis of the obtained models yielded excellent cross-validated q<sup>2</sup>-values of 0.613 (six components) and 0.602 (six components) and non-cross-validated r<sup>2</sup> values of 0.993 and 0.987, respectively. These correlation coefficients suggest that our models are reliable and accurate.

### 6.4. 3D contour maps

To visualize the information content of the derived 3D-QSAR models, CoMFA and CoMSIA contour maps were generated. The contour maps are used to create a “negative” matrix in the place of the unknown active site, and variations of the ligands used can be generated as long as they are better fits in the “imaginary” active site.

**Table 5**  
Inhibitory effects of **8**, **9**, **21**, **23**, **24** and the references NVP and EFV on wild type and NNRTI-resistant HIV-1 replication by cell-based antiviral assay.

Resistance	Compd						
	8	9	21	23	24	NVP	EFV
	IC <sub>50</sub> (μM)	IC <sub>50</sub> (μM)	IC <sub>50</sub> (μM)	IC <sub>50</sub> (μM)	IC <sub>50</sub> (μM)	IC <sub>50</sub> (μM)	IC <sub>50</sub> (μM)
VSVG/HIV <sub>wt</sub> <sup>a</sup>	0.64	0.87	0.062	0.064	0.046	0.031	0.00104
VSVG/HIV <sub>RT-K103N</sub>	8.38 (13) <sup>c</sup>	65.7 (76)	0.54 (8.7)	0.41 (6.4)	0.24 (5.2)	16.1 (519)	0.0588 (56)
VSVG/HIV <sub>RT-Y181C</sub>	6.63 (10)	71.6 (82)	1.26 (20.3)	1.46 (22.8)	0.79 (17.2)	66.7 (2152)	0.00565 (5.4)
VSVG/HIV <sub>RT-L100I,K103N</sub>	NT <sup>b</sup>	NT	5.24 (84.5)	5.36 (83.8)	5.11 (111)	5.0 (161)	2.49 (2394)
VSVG/HIV <sub>RT-Y188L</sub>	NT	NT	>10 (>161)	>10 (>156)	>10 (>217)	>10 (>322)	0.48 (461.5)
VSVG/HIV <sub>RT-K103N,P225H</sub>	NT	NT	4.81 (77.6)	3.59 (56.1)	0.78 (17)	5.48 (177)	0.16 (154)
VSVG/HIV <sub>RT-K103N,G190A</sub>	NT	NT	0.16 (2.6)	0.40 (6.3)	4.18 (90.9)	>10 (>322)	0.056 (538)
VSVG/HIV <sub>RT-K103N,V108I</sub>	NT	NT	4.73 (76.3)	1.84 (28.8)	0.82 (17.8)	2.8 (90)	0.083 (79.8)

<sup>a</sup> VSVG: vesicular stomatitis virus G protein.

<sup>b</sup> NT: not tested.

<sup>c</sup> Mean change (fold) in IC<sub>50</sub> compared to wild type.

### 6.5. CoMFA and CoMSIA contour maps

Fig. 5a and 5b show the electrostatic and steric contour maps of the CoMFA models, respectively. Fig. 5c, 5d, and 5e show the steric-electrostatic, hydrophobic and hydrogen bond donor and acceptor contour maps of the CoMSIA models, respectively. The steric–electrostatic plots of the two models are similar. The electrostatic plot suggests that the electronic plot is consistent with the structure of the TSTs; “N” atoms are near the blue moieties, and “O” atoms are near the red moieties. The steric and hydrophobic plots indicate that the side chain on position 2 of the thiazole is critical; it may be beneficial for the inhibition activity to introduce a bulky group here. This hypothesis can further explain the variation in activity among compounds **6**, **8**, **16** and **20**. Finally, the hydrogen bond donor and acceptor plots suggest the importance of the “N” atom on the thiazole as a hydrogen bond acceptor.

The activities of the training and test sets were also predicted, but the results were not as accurate as we expected. Although the predicted values for the training set are quite consistent with the experimental values, the predicted values for compound **26** are

much higher than the experimental values. However, the values predicted for the other four compounds of the test set are consistent with the experimental values, which indicates that in general, the models can predict the test set well. Compound **26** is the only compound that has a substituted on both the ortho- and meta-moieties. Therefore, this compound may have different interaction mechanisms with the HIV-1 RT that remain unknown (Fig. 6).

### 7. Conclusion

In summary, we have designed a series of 2,4,5-trisubstituted thiazole derivatives (**1–38**) as a novel class of HIV-1 NNRTIs and described an efficient method for their synthesis. Thirty compounds showed potent inhibition of HIV-1 replication at sub-micromolar concentrations against wild type HIV-1 strains. Five of the compounds, **8**, **9**, **21**, **23** and **24**, were also evaluated for their inhibition activity against HIV-1 RT mutants, and compounds **21**, **23** and **24** all showed high levels of inhibition against replication of the most common drug-resistant strains and may have potential as drug candidates for AIDS treatment.

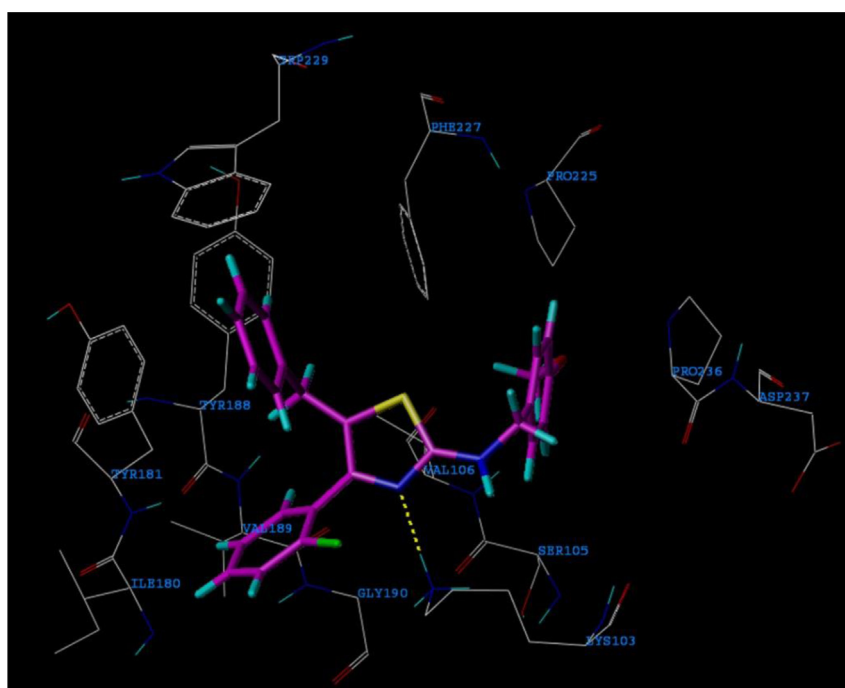


**Fig. 4.** Binding conformation of **24** (magenta) into the NNBS of HIV-1 WT RT (PDB id:2rki). Hydrogen atoms are omitted for clarity. H-Bonds are shown as dotted yellow lines. (For interpretation of the references to color in this figure legend, the reader is referred to the web version of this article.)

**Table 6**  
Summary of CoMFA and CoMSIA statistical analysis.

PLS statistics	CoMFA	CoMSIA
No. compounds	25	25
Optimal number of components (ONC)	6	6
Leave one out $r^2$	0.613	0.602
Std. error of estimate (SEE)	0.064	0.086
Non cross-validated $r^2$	0.993	0.987
$F$ value	487.811	269.361
Steric contribution	0.411	0.112
Electrostatic contribution	0.589	0.352
Hydrophobic contribution	–	0.211
H-bond donor contribution	–	0.186
H-bond acceptor contribution	–	0.139

The result of a docking study revealed the most likely mechanism of interaction between this type of compound and the HIV-1 RT. The 3D-QSAR research also elucidates the SAR and is instructive for further research; for example, it may be beneficial to the inhibition activity to introduce a bulky group on the side chain on

position 2 of the thiazole, and the “N” atom on the thiazole plays an important role as a hydrogen bond acceptor. These results provide future research directions, which are to introduce bulky groups on position 2 and study more substituents on positions 4 and 5 of the thiazole ring.

## 8. Experimental

### 8.1. Chemistry

Starting materials and other reagents were purchased from commercial suppliers and were used without further purification unless otherwise indicated. The melting points were measured with a WRS-1B digital melting point apparatus by Shanghai Measuring Instruments Equipment Co., Ltd.  $^1\text{H}$  NMR spectra were measured on a Mercury 600/300 MHz spectrometer by VARIAN, using TMS as an internal standard.  $^1\text{H}$  NMR spectra were obtained as DMSO- $d_6$  or  $\text{CDCl}_3$  solutions as indicated (reported in ppm). The

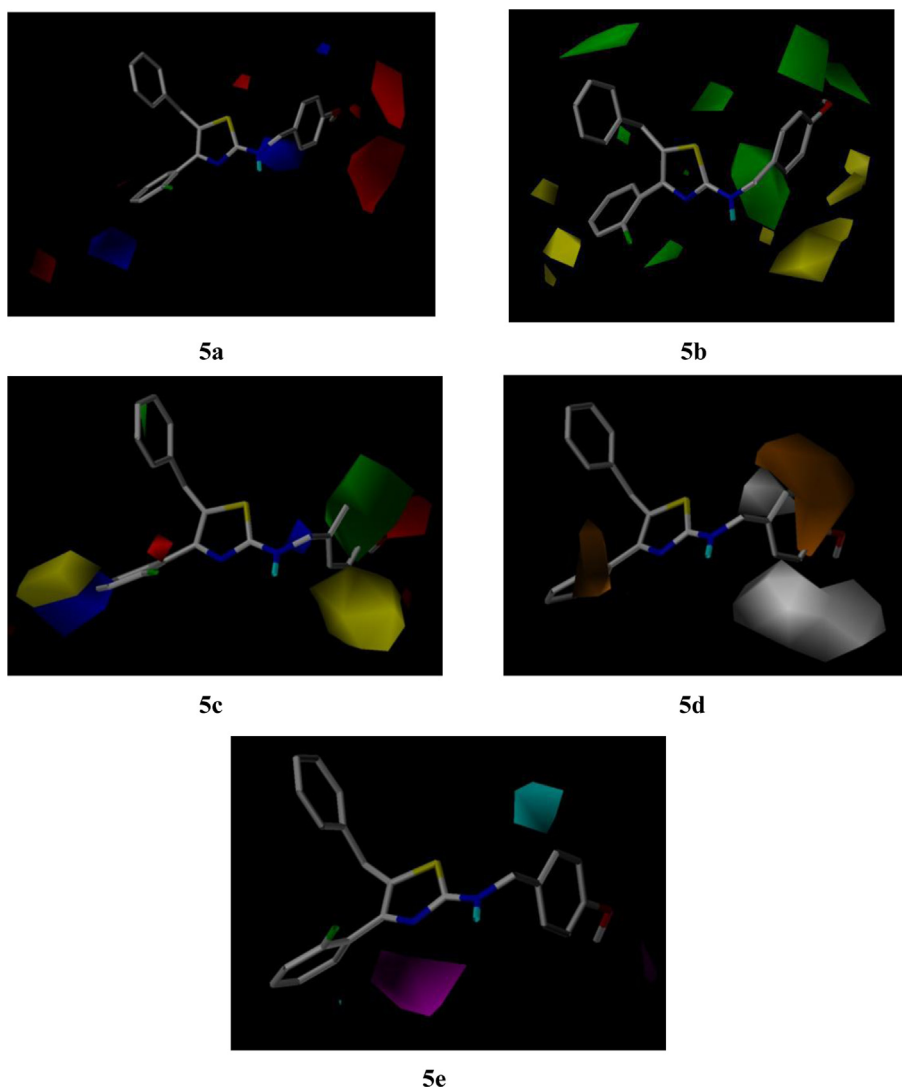


**Fig. 5.** Contour plot of the CoMFA and CoMSIA models. **5a** and **5b** show the steric and electrostatic counter maps of the CoMFA model. Green contours indicate regions where bulky groups increase activity, whereas yellow contours indicate regions where bulky groups decrease activity. Blue contours indicate regions where positive groups increase activity, whereas red contours indicate regions where negative charge increases activity. **5c**, **5d** and **5e** show contour plots of the CoMSIA model. Orange contours indicate regions where hydrophobic groups increase activity, whereas white contours indicate regions where hydrophobic groups decrease activity. Cyan contours indicate regions where H-bond donors increase activity, whereas magenta contours indicate regions where H-bond acceptors increase activity. (For interpretation of the references to color in this figure legend, the reader is referred to the web version of this article.)

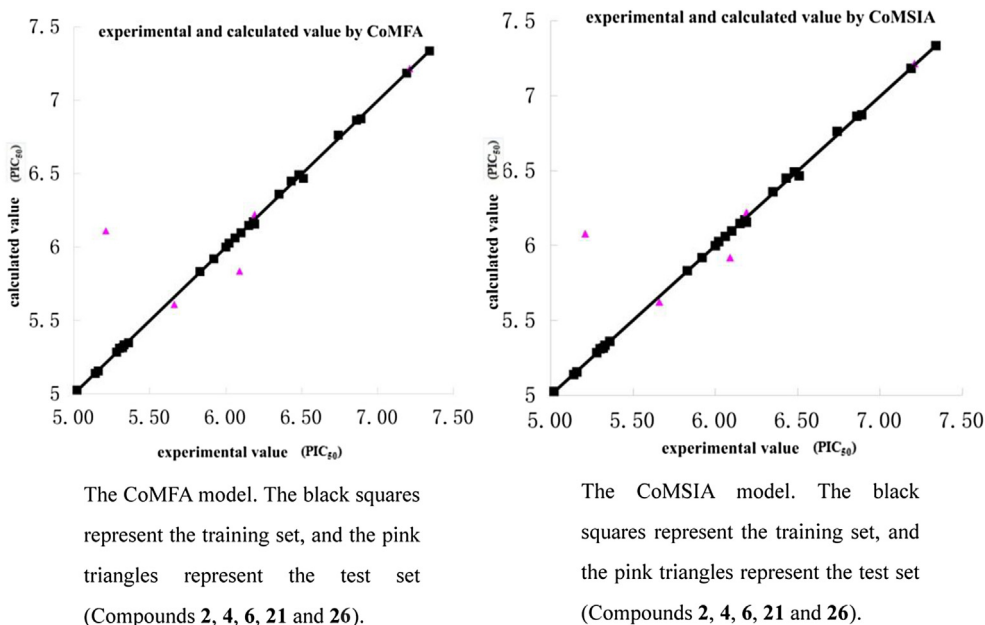


**Fig. 6.** Correlations between the experimental and the predicted activities for the training and test sets for the optimal CoMFA and CoMSIA models, respectively. (For interpretation of the references to color in this figure legend, the reader is referred to the web version of this article.)

mass spectra were obtained using liquid chromatography mass spectrometry (LC-MS) on an APEXIIIFT-ICR mass spectrometer by Bruker with an ESI interface. Thin-layer chromatography (TLC) used silica gel GF254. The hydrogenation reactions were undertaken using a GCD-500 High-purity hydrogen generator and a BLT-2000 medium pressure hydrogenation apparatus produced by Beijing Jiaweikechuang Company. The boiling range for petroleum ether is 60–90 °C. All test compounds showed  $\geq 95\%$  purity as determined by high-performance liquid chromatography (HPLC) except compound **31** with the purity of 92.54%.

## 8.2. General procedure for the preparation of intermediates **39a–39g**, **39i–39k**

The substituted aryl methyl ketone (1.0 mmol), an aqueous solution of 10% sodium hydroxide (2.5 mmol) and ethanol (5 mL) were charged into a 50 mL flask, and the mixture was stirred at room temperature for 10 min, followed by addition of substituted aryl aldehyde (1.05 mmol). The reaction mixture was then stirred at room temperature and monitored using TLC with 5% ethyl acetate/petroleum ether as the solvent system until all reactants disappeared. The mixture was extracted with ethyl acetate three times, and the combined organic phase was dried over sodium sulfate and concentrated under vacuum. The residue was recrystallized from anhydrous ethanol, except for **39i** and **39a**, which were directly used in the next step without purification.

(*E*)-1-(4-methoxyphenyl)-3-phenylprop-2-en-1-one (**39a**) was obtained as a slightly yellow solid in 88% yield.  $^1\text{H NMR}$  (DMSO- $d_6$ , 600 MHz)  $\delta$  3.70 (s, 3H, OCH<sub>3</sub>), 6.98 (d,  $J = 9.0$  Hz, 2H, ArH), 7.43–7.39 (m, 3H, ArH), 7.54 (d,  $J = 15.7$  Hz, 1H, CH=CH), 7.67–7.62 (m, 2H, ArH), 7.79 (d,  $J = 15.7$  Hz, 1H, CH=CH), 8.04 (d,  $J = 9.0$  Hz, 2H, ArH).

(*E*)-1-(2-fluorophenyl)-3-phenylprop-2-en-1-one (**39b**) was obtained as a slightly yellow solid in 83% yield.  $^1\text{H NMR}$  (CDCl<sub>3</sub>, 600 MHz)  $\delta$  7.37–7.33 (m, 2H, ArH), 7.49–7.40 (m, 4H, ArH), 7.64–7.61 (m, 2H, ArH), 7.76–7.72 (m, 3H, ArH).

(*E*)-1,3-bis(4-methoxyphenyl)prop-2-en-1-one (**39c**) was obtained as a white solid in 75% yield, m.p. 98–99 °C.  $^1\text{H NMR}$  (CDCl<sub>3</sub>,

600 MHz)  $\delta$  3.76 (s, 3H, OCH<sub>3</sub>), 3.87 (s, 3H, OCH<sub>3</sub>), 7.56 (d, 1H,  $J = 15.0$  Hz, CH), 7.72 (d, 1H,  $J = 15.0$  Hz, CH), 7.93–6.73 (m, 8H, ArH).

(*E*)-1-(4-fluorophenyl)-3-phenylprop-2-en-1-one (**39d**) was obtained as a white solid in 68% yield, m.p. 81–82 °C.  $^1\text{H NMR}$  (CDCl<sub>3</sub>, 600 MHz)  $\delta$  7.50 (d, 1H,  $J = 16.0$  Hz, CH), 7.82 (d, 1H,  $J = 16.0$  Hz, CH), 8.07–7.16 (m, 9H, ArH).

(*E*)-1-(2,4-difluorophenyl)-3-phenylprop-2-en-1-one (**39e**) was obtained as a slightly yellow solid in 93% yield.  $^1\text{H NMR}$  (DMSO- $d_6$ , 600 MHz)  $\delta$  6.91 (ddd,  $J_1 = 10.9$  Hz,  $J_2 = 8.7$  Hz,  $J_3 = 2.4$  Hz, 1H, ArH), 7.00 (td,  $J_1 = 7.8$  Hz,  $J_2 = 2.4$  Hz, 1H, ArH), 7.39 (dd,  $J_1 = 15.6$  Hz,  $J_2 = 3.0$ , 1H, CH=CH), 7.44–7.40 (m, 3H, ArH), 7.65–7.61 (m, 2H, ArH), 7.77 (dd,  $J_1 = 15.6$  Hz,  $J_2 = 1.9$  Hz, 2H, CH=CH), 7.89 (td,  $J_1 = 8.5$  Hz,  $J_2 = 6.5$  Hz, 1H, ArH).

(*E*)-1-(2-chlorophenyl)-3-phenylprop-2-en-1-one (**39f**) was obtained as a slightly yellow oil in 95% yield.  $^1\text{H NMR}$  (DMSO- $d_6$ , 600 MHz)  $\delta$  7.14 (d,  $J = 16.1$ , 1H, CH=CH), 7.37 (td, 1H,  $J_1 = 7.4$  Hz,  $J_2 = 1.3$  Hz, ArH), 7.42–7.39 (m, 3H, ArH), 7.43 (dd, 1H,  $J_1 = 7.4$  Hz,  $J_2 = 1.8$  Hz, ArH), 7.50–7.43 (m, 3H, ArH), 7.59–7.55 (m, 2H, ArH).

(*E*)-1-(2,4-dichlorophenyl)-3-phenylprop-2-en-1-one (**39g**) was obtained as a slightly yellow oil in 63% yield.  $^1\text{H NMR}$  (DMSO- $d_6$ , 600 MHz)  $\delta$  7.12 (dd,  $J_1 = 16.0$  Hz,  $J_2 = 0.9$  Hz, 1H, CH=CH), 7.36 (ddd, 1H,  $J_1 = 8.2$  Hz,  $J_2 = 2.0$  Hz,  $J_3 = 0.9$  Hz, ArH), 7.44–7.41 (m, 5H, ArH, CH=CH), 7.49 (dd,  $J_1 = 2.3$  Hz,  $J_2 = 1.3$  Hz, 1H, ArH), 7.59–7.55 (m, 2H, ArH).

(*E*)-3-(2-methoxyphenyl)-1-phenylprop-2-en-1-one (**39j**) was obtained as a slightly yellow solid in 90%, m.p. 56.4–56.8 °C. IR (KBr,  $\text{cm}^{-1}$ ): 3103, 3030, 1660 ( $\nu_{\text{CO}}$ ), 1600, 1488, 1341, 1315, 1248, 1180, 1017, 754, 730;  $^1\text{H NMR}$  (CDCl<sub>3</sub>, 600 MHz)  $\delta$  3.94 (s, 3H, CH<sub>3</sub>O), 6.97 (d,  $J = 7.80$  Hz, 1H, ArH), 7.02 (t,  $J = 7.80$  Hz, 1H, ArH), 7.41 (d,  $J = 7.20$  Hz, 1H, ArH), 7.52 (t,  $J = 7.80$  Hz, 2H, ArH), 7.58 (t,  $J = 7.80$  Hz, 1H, ArH), 7.66 (d,  $J = 15.60$  Hz, 1H, CH=CH), 7.67 (d,  $J = 7.20$  Hz, 1H, ArH), 8.04 (d,  $J = 7.80$  Hz, 2H, ArH), 8.14 (d,  $J = 15.60$  Hz, 1H, CH=CH). IR (KBr,  $\text{cm}^{-1}$ ): 3103, 3030, 1660 ( $\nu_{\text{C=O}}$ ), 1600, 1488, 1341, 1315, 1248, 1180, 1017, 754, 730.

(*E*)-4-(3-oxo-3-phenylprop-1-enyl)benzoxonitrile (**39k**) was obtained as a slightly yellow solid in 83.7% yield, m.p. 153.6–153.8 °C.  $^1\text{H NMR}$  (CDCl<sub>3</sub>, 600 MHz)  $\delta$  7.53 (t,  $J = 7.8$  Hz, 2H, ArH), 7.61 (d,  $J = 15.6$  Hz, 1H, CH=CH), 7.62 (t, 1H, ArH), 7.23 (q, 4H, ArH), 7.78 (d,  $J = 15.6$  Hz, 1H, CH=CH), 8.03 (d,  $J = 7.8$  Hz, 2H, ArH). IR (KBr,

$\text{cm}^{-1}$ ): 3061, 2221, 1662 ( $\nu_{\text{C}=\text{O}}$ ), 1603, 1577, 1558, 1335, 1221, 1015, 988, 833, 778, 726, 694.

### 8.3. General procedure for the preparation of intermediates **40a–40m, 44a**

The chalcone, Pd/C (an amount equal to  $\frac{1}{4}$  the quantity of the chalcone) and 30 mL of ethyl acetate were placed into the reactor. The reaction was conducted in an BLT-2000 medium-pressure hydrogenation apparatus for 3.5–4 h and monitored by TLC using 5% ethyl acetate/petroleum ether as the solvent system. When the reaction was finished, the Pd/C was filtered, and the solvent was removed. In most cases, the crude product was purified by column chromatography using ethyl acetate/petroleum ether as the solvent system. Compounds **40e**, **40i**, and **40j** were obtained as pure products monitored by TLC, and the crude products were directly used in the next step.

**1-(4-methoxyphenyl)-3-phenylpropan-1-one (40a)** was obtained as a white solid in 95% yield, m.p. 96.5–97.2 °C.  $^1\text{H NMR}$  ( $\text{CDCl}_3$ , 400 MHz)  $\delta$  3.05 (t,  $J = 8.16$  Hz, 2H,  $\text{ArCH}_2$ ), 3.25 (t,  $J = 8.16$  Hz, 2H,  $\text{COCH}_2$ ), 3.86 (s, 3H,  $\text{OCH}_3$ ), 6.92 (d,  $J = 9.00$  Hz, 2H, ArH), 7.32–7.18 (5H, m, ArH), 7.94 (d,  $J = 9.00$  Hz, 2H, ArH). EI-MS  $m/z$  240.1 [ $\text{M}^+$ , 37], 135 (100).

**1-(2-fluorophenyl)-3-phenylpropan-1-one (40b)** was obtained as a colorless oil in 94% yield.  $^1\text{H NMR}$  ( $\text{CDCl}_3$ , 400 MHz)  $\delta$  2.93 (t,  $J = 7.5$  Hz, 2H,  $\text{CH}_2$ ), 3.30 (td,  $J_1 = 7.5$ ,  $J_2 = 2.4$  Hz, 2H,  $\text{CH}_2$ ), 7.18 (td,  $J_1 = 6.9$ ,  $J_2 = 1.7$  Hz, 1H, ArH), 7.28–7.23 (m, 4H, ArH), 7.36–7.33 (m, 2H, ArH), 7.66–7.64 (m, 1H, ArH), 7.83 (td,  $J_1 = 7.7$ ,  $J_2 = 1.7$  Hz, 1H, ArH).

**1,3-bis(4-methoxyphenyl)propan-1-one (40c)** was obtained as a clear solid in 78% yield, m.p. 85–86 °C.  $^1\text{H NMR}$  ( $\text{CDCl}_3$ , 600 MHz)  $\delta$  2.99 (t, 2H,  $\text{CH}_2$ ), 3.21 (t, 2H,  $\text{CH}_2$ ), 3.80 (s, 3H,  $\text{OCH}_3$ ), 3.86 (s, 3H,  $\text{OCH}_3$ ), 6.83 (d,  $J = 8.4$  Hz, 2H, ArH), 6.92 (d,  $J = 9.0$  Hz, 2H, ArH), 7.16 (d,  $J = 9.0$  Hz, 2H, ArH), 7.94 (d,  $J = 8.4$  Hz, 2H, ArH).

**1-(4-fluorophenyl)-3-phenylpropan-1-one (40d)** was obtained as a clear solid in 94% yield.  $^1\text{H NMR}$  ( $\text{CDCl}_3$ , 600 MHz)  $\delta$  3.06 (t,  $J = 7.7$  Hz, 2H,  $\text{CH}_2$ ), 3.27 (t,  $J = 7.7$  Hz, 2H,  $\text{CH}_2$ ), 7.11 (t,  $J = 8.4$  Hz, 2H, ArH), 7.29–7.20 (m, 5H, ArH), 7.99–7.96 (m, 2H, ArH).

**1-(2-chlorophenyl)-3-phenylpropan-1-one (40f)** was obtained as slightly yellow oil in 53% yield.  $^1\text{H NMR}$  ( $\text{DMSO}-d_6$ , 600 MHz)  $\delta$  3.05 (t,  $J = 7.8$  Hz, 2H,  $\text{CH}_2$ ), 3.27 (t,  $J = 7.2$  Hz, 2H,  $\text{CH}_2$ ), 7.24–7.20 (m, 3H, ArH), 7.31–7.27 (m, 3H, ArH), 7.37 (tt, 1H,  $J_1 = 7.9$  Hz,  $J_2 = 1.7$  Hz, ArH), 7.41–7.39 (m, 2H, ArH).

**1-(2,4-dichlorophenyl)-3-phenylpropan-1-one (40g)** was obtained as a clear oil in 85% yield.  $^1\text{H NMR}$  ( $\text{DMSO}-d_6$ , 600 MHz)  $\delta$  3.05 (t,  $J = 7.8$  Hz, 2H,  $\text{CH}_2$ ), 3.26 (t,  $J = 7.8$  Hz, 2H,  $\text{CH}_2$ ), 7.23–7.20 (m, 3H, ArH), 7.31–7.27 (m, 3H, ArH), 7.37 (d,  $J = 8.3$ , 1H, ArH), 7.43 (d,  $J = 1.9$ , 1H, ArH).

**1-(2,5-dimethoxyphenyl)-3-phenylpropan-1-one (40h)** was obtained as a white solid in 77% yield, m.p. 54.7–56.7 °C.  $^1\text{H NMR}$  ( $\text{CDCl}_3$ , 400 MHz)  $\delta$  3.05 (t,  $J = 8.16$  Hz, 2H,  $\text{ArCH}_2$ ), 3.25 (t,  $J = 8.16$  Hz, 2H,  $\text{COCH}_2$ ), 3.86 (s, 3H,  $\text{OCH}_3$ ), 3.95 (s, 3H,  $\text{OCH}_3$ ), 7.94–6.92 (m, 8H, ArH).

**4-(3-oxo-3-phenylpropyl)benzoxonitrile (40k)** was obtained as a white solid in 99.2% yield, m.p. 77.5–77.9 °C.  $^1\text{H NMR}$  ( $\text{CDCl}_3$ , 600 MHz)  $\delta$  3.14 (t,  $J = 7.2$  Hz, 2H,  $\text{CH}_2\text{CH}_2$ ), 3.33 (t,  $J = 7.2$  Hz, 2H,  $\text{CH}_2\text{CH}_2$ ), 7.37 (d,  $J = 8.4$  Hz, 2H, ArH), 7.47 (t,  $J = 8.4$  Hz, 2H, ArH), 7.60–7.56 (m, 3H, ArH), 7.95 (d,  $J = 8.4$  Hz, 2H, ArH). IR (KBr,  $\text{cm}^{-1}$ ): 3066, 3960, 2903, 2220, 1679 ( $\nu_{\text{C}=\text{O}}$ ), 1604, 1446, 1211, 828, 787, 747, 690.

**1-(4-methoxyphenyl)-3-(4-nitrophenyl)propan-1-one (40l)** it was obtained as a white solid in 83% yield, m.p. 123–125 °C.  $^1\text{H NMR}$  ( $\text{CDCl}_3$ , 400 MHz)  $\delta$  3.18 (t,  $J = 7.00$  Hz, 2H,  $\text{CH}_2$ ), 3.30 (t,  $J = 7.00$  Hz, 2H,  $\text{CH}_2$ ), 3.87 (3H, s,  $\text{OCH}_3$ ), 6.93 (d,  $J = 8.96$  Hz, 2H, ArH), 7.42 (d,  $J = 8.60$  Hz, 2H, ArH), 7.93 (d,  $J = 8.96$  Hz, 2H,

ArH), 8.15 (d,  $J = 8.60$  Hz, 2H, ArH); EI-MS  $m/z$  285.0 [ $\text{M}^+$ , 62], 134 (100).

**3-(4-fluorophenyl)-1-(4-methoxyphenyl)propan-1-one (40m)** was obtained as a white solid in 80% yield, m.p. 72–73 °C.  $^1\text{H NMR}$  ( $\text{CDCl}_3$ , 600 MHz)  $\delta$  3.02 (t,  $J = 7.2$  Hz, 2H,  $\text{CH}_2$ ), 3.22 (t,  $J = 7.2$  Hz, 2H,  $\text{CH}_2$ ), 3.86 (s, 3H,  $\text{OCH}_3$ ), 6.91 (d,  $J = 9.0$  Hz, 2H, ArH), 6.97 (t,  $J = 8.4$  Hz, 2H, ArH), 7.21–7.19 (m, 2H, ArH), 7.93 (d,  $J = 8.4$  Hz, 2H, ArH).

**1-(furan-2-yl)-3-phenylpropan-1-one (44a)** was obtained as a clear solid in 99% yield, m.p. 76–77 °C.  $^1\text{H NMR}$  ( $\text{CDCl}_3$ , 600 MHz)  $\delta$  3.04 (t,  $J = 7.8$  Hz, 2H,  $\text{CH}_2$ ), 3.15 (t,  $J = 7.8$  Hz, 2H,  $\text{CH}_2$ ), 6.52–6.50 (m, 1H, ArH), 7.16 (d,  $J = 3.6$  Hz, 1H, ArH), 7.20 (t,  $J = 7.2$  Hz, 1H, ArH), 7.24 (t,  $J = 6.6$  Hz, 2H, ArH), 7.30 (t,  $J = 7.2$  Hz, 2H, ArH), 7.56 (s, 1H, ArH).

### 8.4. General procedure for the preparation of intermediates **42a–42m, 45a and 45b**

To obtain **41a–41m**, in a 50 mL three-necked flask, the reduction product from the previous step, a catalytic amount of aluminum trichloride and 10 mL of chloroform were added. Then, bromine (1 equivalent) dissolved in 10 mL of chloroform was added dropwise at room temperature. After addition was complete, the mixture was stirred for 6 h at room temperature and then transferred to a separatory funnel; extracted with dichloromethane; washed with water, saturated sodium carbonate and saturated sodium chloride; dried over anhydrous sodium sulfate overnight; filtered; and concentrated under reduced pressure to give the crude product. In most cases, TLC showed that the product was nearly pure, thus, the crude residue could be used directly in the next step without further purification except for **41a** and **41h**. In some examples, the crude product was purified by column chromatography on silica gel using petroleum ether/ethyl acetate as eluent.

The bromide **41a–41m** obtained from the previous step, thio-urea (1 equivalent), anhydrous sodium acetate (1 equivalent) and 15 mL of anhydrous ethanol were placed into a 50 mL round-bottom flask. The mixture was refluxed for 5–8 h and cooled to room temperature. Then, the solvent was removed, and the mixture was extracted with ethyl acetate, washed with water, saturated sodium carbonate and saturated sodium chloride, dried over anhydrous sodium sulfate, and concentrated over vacuum. The crude product was purified by column chromatography on silica gel using petroleum ether/ethyl acetate as eluent to afford intermediates **42a–42m, 45a and 45b**.

**2-bromo-1-(4-methoxyphenyl)-3-phenylpropan-1-one (41a)** was obtained as a white solid in 98.9% yield, m.p. 57.4–58.3 °C.  $^1\text{H NMR}$  ( $\text{CDCl}_3$ , 400 MHz)  $\delta$  3.34 (dd,  $J_1 = 14.28$  Hz,  $J_2 = 7.00$  Hz, 1H,  $\text{ArCH}_2$ ), 3.66 (dd,  $J_1 = 14.28$  Hz,  $J_2 = 7.00$  Hz, 1H,  $\text{ArCH}_2$ ), 3.13 (s, 3H,  $\text{OCH}_3$ ), 5.29 (t,  $J = 7.32$  Hz, 1H,  $\text{CHBr}$ ), 6.91 (d,  $J = 9.00$  Hz, 2H, ArH), 7.32–7.18 (m, 5H, ArH), 7.94 (d,  $J = 9.00$  Hz, 2H, ArH); ESI-MS  $m/z$  320.8 [ $\text{M}^+$ , 100], 239.2 [ $\text{M}-\text{Br}$ , 18].

**2-bromo-1-(2,5-dimethoxyphenyl)-3-phenylpropan-1-one (41h)** was obtained as a white solid in 48% yield, m.p. 79.4–80.1 °C.  $^1\text{H NMR}$  ( $\text{CDCl}_3$ , 300 MHz)  $\delta$  3.26 (dd,  $J_1 = 14.28$  Hz,  $J_2 = 7.50$  Hz, 1H,  $\text{ArCH}_2$ ), 3.66 (dd,  $J_1 = 14.28$  Hz,  $J_2 = 7.50$  Hz, 1H,  $\text{ArCH}_2$ ), 3.69 (s, 3H,  $\text{OCH}_3$ ), 3.79 (s, 3H,  $\text{OCH}_3$ ), 5.66 (t,  $J = 7.32$  Hz, 1H, 6.86–7.31 (m, 8H, ArH).

**5-benzyl-4-(4-methoxyphenyl)thiazol-2-amine (42a)** was obtained as a slightly yellow solid in 98.6% yield, m.p. 177–178 °C.  $^1\text{H NMR}$  ( $\text{DMSO}-d_6$ , 400 MHz)  $\delta$  3.76 (s, 3H,  $\text{OCH}_3$ ), 4.04 (s, 2H,  $\text{CH}_2$ ), 6.82 (s, 2H,  $\text{NH}_2$ ), 6.93 (d,  $J = 9.00$  Hz, 2H, ArH), 7.18–7.35 (m, 5H, ArH), 7.46 (d,  $J = 9.00$  Hz, 2H, ArH). EI-MS  $m/z$  296.1 [ $\text{M}^+$ , 100], 219.0 (19); HREI-MS Calcd. for  $\text{C}_{17}\text{H}_{16}\text{N}_2\text{OS}$  296.0983, found 296.0978.

**5-benzyl-4-(2-fluorophenyl)thiazol-2-amine (42b)** was obtained as a slightly yellow oil in 35% yield.  $^1\text{H NMR}$  ( $\text{DMSO}-d_6$ , 600 MHz)  $\delta$  3.80 (s, 2H,  $\text{CH}_2$ ), 6.84 (s, 2H,  $\text{NH}_2$ ), 7.10 (d,  $J = 7.2$ , 2H, ArH), 7.17 (t,  $J = 7.2$  Hz, 1H, ArH), 7.22–7.27 (m, 4H, ArH), 7.41 (m, 2H, ArH). ESI-MS  $m/z$  285 [ $\text{M}^+$ ].

5-(4-methoxybenzyl)-4-(4-methoxyphenyl)thiazol-2-amine (**42c**) was obtained as a slightly yellow solid in 73% yield, m.p. 182–183 °C. <sup>1</sup>H NMR (DMSO-*d*<sub>6</sub>, 600 MHz) δ 3.72 (s, 3H, OCH<sub>3</sub>), 3.76 (s, 3H, OCH<sub>3</sub>), 3.96 (s, 2H, ArCH<sub>2</sub>), 6.77 (s, 2H, NH<sub>2</sub>), 6.87 (d, *J* = 8.40 Hz, 2H, ArH), 6.93 (d, *J* = 9.00 Hz, 2H, ArH), 7.10 (d, *J* = 9.00 Hz, 2H, ArH), 7.46 (d, *J* = 8.40 Hz, 2H, ArH).

5-benzyl-4-(4-fluorophenyl)thiazol-2-amine (**42d**) was obtained as a slightly yellow solid in 60% yield. IR (KBr, cm<sup>-1</sup>): 3433 (NH), 3270 (NH), 2365, 1620, 1500, 1333, 1224, 844; <sup>1</sup>H NMR (DMSO-*d*<sub>6</sub>, 600 MHz) δ 4.05 (s, 2H, ArCH<sub>2</sub>), 6.86 (s, 2H, NH<sub>2</sub>), 7.19–7.23 (m, 5H, ArH), 7.31 (q, 2H, ArH), 7.56 (q, 2H, ArH).

5-benzyl-4-(2,4-difluorophenyl)thiazol-2-amine (**42e**) was obtained as a yellow solid in 75% yield. <sup>1</sup>H NMR (DMSO-*d*<sub>6</sub>, 600 MHz) δ 3.77 (s, 2H, CH<sub>2</sub>), 6.84 (s, 2H, NH<sub>2</sub>), 7.09–7.11 (m, 3H, ArH), 7.16 (t, *J* = 7.8 Hz, 1H, ArH), 7.24–7.27 (m, 3H, ArH), 7.45 (q, *J* = 7.8 Hz, 1H, ArH). ESI-MS *m/z* 303 [M+H]<sup>+</sup>.

5-benzyl-4-(2-chlorophenyl)thiazol-2-amine (**42f**) was obtained as a yellow solid in 62% yield. <sup>1</sup>H NMR (DMSO-*d*<sub>6</sub>, 600 MHz) δ 3.77 (s, 2H, CH<sub>2</sub>), 6.88 (s, 2H, NH<sub>2</sub>), 7.14 (d, *J* = 7.2 Hz, 2H, ArH), 7.22 (t, *J* = 7.2 Hz, 2H, ArH), 7.30 (t, *J* = 7.2 Hz, 2H, ArH), 7.42–7.45 (m, 3H, ArH), 7.58 (d, *J* = 7.8, 1H, ArH). ESI-MS *m/z* 301 [M+H]<sup>+</sup>.

5-benzyl-4-(2,4-dichlorophenyl)thiazol-2-amine (**42g**) was obtained as a slightly yellow solid in 43% yield. <sup>1</sup>H NMR (DMSO-*d*<sub>6</sub>, 600 MHz) δ 3.83 (s, 2H, CH<sub>2</sub>), 7.01 (s, 2H, NH<sub>2</sub>), 7.20 (d, *J* = 7.8 Hz, 2H, ArH), 7.28 (t, *J* = 7.2 Hz, 1H, ArH), 7.36 (t, *J* = 7.2 Hz, 2H, ArH), 7.52 (d, *J* = 8.4 Hz, 1H, ArH), 7.56–7.58 (m, 1H, ArH), 7.80 (d, *J* = 1.8 Hz, 1H, ArH). ESI-MS *m/z* 335 [M+H]<sup>+</sup>.

5-benzyl-4-(2,5-dimethoxyphenyl)thiazol-2-amine (**42h**) was obtained as a white solid in 69% yield, m.p. 144.1–144.8 °C. <sup>1</sup>H NMR (DMSO-*d*<sub>6</sub>, 300 MHz) δ 3.65 (s, 3H, OCH<sub>3</sub>), 3.68 (s, 3H, OCH<sub>3</sub>), 3.73 (s, 2H, CH<sub>2</sub>), 6.74–7.29 (m, 8H, ArH).

5-benzyl-4-phenylthiazol-2-amine (**42i**) was obtained as a slightly yellow solid in 73% yield, m.p. 165–166 °C. <sup>1</sup>H NMR (DMSO-*d*<sub>6</sub>, 600 MHz) δ 4.06 (s, 2H, ArCH<sub>2</sub>), 6.85 (s, 2H, NH<sub>2</sub>), 7.19–7.21 (m, 3H, ArH), 7.30–7.32 (m, 3H, ArH), 7.38 (t, *J* = 7.2 Hz, 2H, ArH), 7.55 (d, *J* = 7.2 Hz, 2H, ArH).

5-(2-methoxybenzyl)-4-phenylthiazol-2-amine (**42j**) was obtained as a yellow solid in 66.2% yield. <sup>1</sup>H NMR (DMSO-*d*<sub>6</sub>, 600 MHz) δ 3.76 (s, 3H, CH<sub>3</sub>O), 3.97 (s, 2H, CH<sub>2</sub>), 6.79 (s, 2H, NH<sub>2</sub>), 6.89 (t, *J* = 7.2 Hz, 1H, ArH), 6.99 (d, *J* = 8.4 Hz, 1H, ArH), 7.07 (d, *J* = 7.2 Hz, 1H, ArH), 7.23 (t, *J* = 7.8 Hz, 1H, ArH), 7.28 (t, *J* = 7.2 Hz, 1H, ArH), 7.37 (t, *J* = 7.8 Hz, 2H, ArH), 7.53 (d, *J* = 7.8 Hz, 2H, ArH). IR (KBr, cm<sup>-1</sup>): 3428, 3276 (ν<sub>N-H</sub>), 3135, 2955, 2838, 1623, 1597, 1526, 1488, 1293, 1245, 1031, 779, 755, 702.

4-((2-amino-4-phenylthiazol-5-yl)methyl)benzotrile (**42k**) was obtained as a slightly yellow solid in 55.9% yield. <sup>1</sup>H NMR (DMSO-*d*<sub>6</sub>, 600 MHz) δ 4.17 (s, 2H, CH<sub>2</sub>), 6.93 (s, 2H, NH<sub>2</sub>), 7.30 (t, *J* = 7.2 Hz, 1H, ArH), 7.36–7.40 (m, 4H, ArH), 7.50 (d, *J* = 7.8 Hz, 2H, ArH), 7.78 (d, *J* = 7.8 Hz, 2H, ArH).

4-(4-methoxyphenyl)-5-(4-nitrobenzyl)thiazol-2-amine (**42l**) was obtained as a white solid in 69% yield, m.p. 209–210 °C. <sup>1</sup>H NMR (DMSO-*d*<sub>6</sub>, 400 MHz) δ 3.34 (s, 3H, OCH<sub>3</sub>), 4.20 (s, 2H, CH<sub>2</sub>), 6.93 (s, 2H, NH<sub>2</sub>), 6.95 (d, *J* = 8.72 Hz, 2H, ArH), 7.43–7.46 (m, 4H, ArH), 8.19 (d, *J* = 8.72 Hz, 2H, ArH); EI-MS *m/z* 341.2 [M<sup>+</sup>, 100], 219.1 (14); HREI-MS Calcd. for C<sub>17</sub>H<sub>15</sub>N<sub>3</sub>O<sub>3</sub>S 341.0834, found 341.0834.

5-(4-fluorobenzyl)-4-(4-methoxyphenyl)thiazol-2-amine (**42m**) was obtained as a white solid in 82% yield, m.p. 181–182 °C. <sup>1</sup>H NMR (DMSO-*d*<sub>6</sub>, 600 MHz) δ 3.74 (s, 3H, OCH<sub>3</sub>), 4.01 (s, 2H, ArCH<sub>2</sub>), 6.80 (s, 2H, NH<sub>2</sub>), 6.92 (d, *J* = 9.00 Hz, 2H, ArH), 7.11 (t, 2H, ArH), 7.20 (q, 2H, ArH), 7.43 (d, *J* = 9.00 Hz, 2H, ArH); ESI-MS *m/z* 315[M+H]<sup>+</sup>.

5-benzyl-4-(furan-2-yl)thiazol-2-amine (**45a**) was obtained as a slightly yellow solid 78%, m.p. 171–172 °C. <sup>1</sup>H NMR (DMSO-*d*<sub>6</sub>, 600 MHz) δ 4.24 (s, 2H, ArCH<sub>2</sub>), 6.90 (s, 2H, NH<sub>2</sub>), 6.53–7.68 (m, 8H, ArH); Calcd. For C<sub>14</sub>H<sub>12</sub>N<sub>2</sub>O<sub>2</sub>S: 256, ESI-MS *m/z* 257 [M+H]<sup>+</sup>.

4-(4-methoxyphenyl)-5-methylthiazol-2-amine (**45b**) was obtained as a yellow solid in 84% yield, m.p. 131–132 °C. <sup>1</sup>H NMR (DMSO-*d*<sub>6</sub>, 600 MHz) δ 2.28 (s, 3H, CH<sub>3</sub>), 3.77 (s, 3H, OCH<sub>3</sub>), 6.71 (s, 2H, NH<sub>2</sub>), 6.93 (d, *J* = 8.4 Hz, 2H, ArH), 7.48 (d, *J* = 8.4 Hz, 2H, ArH).

### 8.5. General procedure for the preparation of compounds 1–3

Compound **43** and DMF (or diethylamine) were added to a 100 mL round-bottom flask and stirred for 12 h at 120 °C, and the reaction was monitored by TLC until completed. Then, the solvent was removed, and the mixture was extracted with ethyl acetate; washed with water, saturated sodium carbonate and saturated sodium chloride, dried over anhydrous sodium sulfate, and concentrated over vacuum. The crude product was purified by column chromatography on silica gel using petroleum ether/ethyl acetate as eluent to obtain **1** and **2**. To a 100 mL three-necked flask, **2** (0.5 g, 0.763 mmol) and CH<sub>2</sub>Cl<sub>2</sub> (40 mL) were added. Then, the mixture was cooled to –20 °C, and BBr<sub>3</sub>/CH<sub>2</sub>Cl<sub>2</sub> 8 mL (8 mmol) solution was added dropwise and stirred for 1 h. The mixture was stirred at room temperature for 2 h, and 8 g of ice was added. The formed precipitate was filtrated to afford compound **3**, as a yellow solid.

5-benzyl-4-(4-methoxyphenyl)-*N,N*-dimethylthiazol-2-amine (**1**) was obtained as a white solid in 21.4% yield, m.p. 121.1–122.0 °C. <sup>1</sup>H NMR (CDCl<sub>3</sub>, 300 MHz) δ 3.04 (s, 6H, N,N (CH<sub>3</sub>)<sub>2</sub>), 3.84 (s, 3H, OCH<sub>3</sub>), 4.21 (s, 2H, CH<sub>2</sub>), 6.95 (d, *J* = 8.96 Hz, 2H, ArH), 7.18–7.38 (m, 5H, ArH), 7.54 (d, *J* = 8.96 Hz, 2H, ArH); <sup>13</sup>C NMR (151 MHz, CDCl<sub>3</sub>) δ 168.23, 158.94, 148.07, 140.88, 129.72, 128.48, 128.20, 126.39, 118.72, 113.71, 55.28, 40.05, 33.03; ESI-MS *m/z* 325 [M+H]<sup>+</sup>.

5-benzyl-*N,N*-diethyl-4-(4-methoxyphenyl)thiazol-2-amine (**2**) was obtained as a white solid in 63.1% yield, m.p. 83.2–83.6 °C. <sup>1</sup>H NMR (CDCl<sub>3</sub>, 300 MHz) δ 1.22 (t, *J* = 7.2 Hz, 6H, 2 × CH<sub>3</sub>), 3.46 (q, *J* = 7.2 Hz, 4H, 2 × CH<sub>2</sub>), 3.81 (s, 3H, OCH<sub>3</sub>), 4.10 (s, 2H, ArCH<sub>2</sub>), 6.8–6.92 (m, 2H, ArH) 7.22–7.34 (m, 5H, ArH) 7.52–7.57 (m, 2H, ArH); <sup>13</sup>C NMR (151 MHz, CDCl<sub>3</sub>) δ 166.60, 158.85, 140.92, 129.68, 128.50, 128.22, 126.32, 117.32, 113.63, 55.26, 44.90, 33.02, 12.71; ESI-MS *m/z* 353 [M+H]<sup>+</sup>.

4-(5-benzyl-2-(diethylamino)thiazol-4-yl)phenol (**3**) was obtained as a slightly yellow solid in 18.8% yield, m.p. 173.1–174.5 °C. <sup>1</sup>H NMR (DMSO-*d*<sub>6</sub>, 600 MHz) δ 1.19 (t, *J* = 6.9 Hz, 6H, 2 × CH<sub>3</sub>), 3.55 (q, *J* = 6.9 Hz, 4H, 2 × CH<sub>2</sub>), 3.99 (s, 2H, ArCH<sub>2</sub>), 6.92 (d, *J* = 8.2 Hz, 2H, ArH), 7.23–7.20 (m, 2H, ArH), 7.28–7.23 (m, 1H, ArH), 7.33 (t, *J* = 7.6 Hz, 2H, ArH), 7.41–7.37 (m, 2H, ArH), 9.90 (s, 1H, OH); <sup>13</sup>C NMR (151 MHz, CDCl<sub>3</sub>) δ 165.58, 158.86, 137.90, 137.51, 131.14, 129.06, 128.37, 127.43, 117.53, 115.77, 32.35, 30.94, 12.43; ESI-MS *m/z* 339[M+H]<sup>+</sup>.

### 8.6. General procedure for the preparation of compounds 4–36 and the paraperation of compounds 37,38

The 4,5-disubstituted thiazol-2-amine obtained from the previous step, a substituted aryl aldehyde (1 equivalent) and a catalytic amount of *p*-toluenesulfonic acid were added into a 50 mL round-bottom flask, and the mixture was refluxed in toluene for 24 h. Then, the solvent was removed, and sodium borohydride (5 equivalent) in ethanol was added. Further purification of compound **36** was performed using column chromatography to afford the pure product. For the other compounds, the mixture was stirred for 2–3 h and monitored by TLC. After the solvent was removed and the mixture was extracted, washed and concentrated, column chromatography was performed for further purification.

*N*,5-dibenzyl-4-(4-methoxyphenyl)thiazol-2-amine (**4**) was obtained as a white solid in 95% yield, m.p. 145.7–146.5 °C. <sup>1</sup>H NMR (CDCl<sub>3</sub>, 600 MHz) δ 3.86 (s, 3H, OCH<sub>3</sub>), 4.09 (d, 2H, *J* = 6.0 Hz, ArCH<sub>2</sub>), 4.40 (s, 2H, ArCH<sub>2</sub>), 6.95 (dd, *J*<sub>1</sub> = 8.4 Hz, *J*<sub>2</sub> = 1.2 Hz, 2H,

ArH), 7.28–7.17 (m, 4H, ArH), 7.38–7.28 (m, 6H, ArH), 7.51–7.45 (m, 2H, ArH), 7.93 (t,  $J = 5.9$  Hz, NH);  $^{13}\text{C}$  NMR (151 MHz,  $\text{CDCl}_3$ )  $\delta$  167.06, 159.01, 140.56, 137.81, 129.65, 128.62, 128.56, 128.16, 127.54, 126.46, 113.71, 55.24, 49.73, 32.91; ESI-MS  $m/z$  387  $[\text{M}+\text{H}]^+$ .

5-benzyl-N-(2-methoxybenzyl)-4-(4-methoxyphenyl)thiazol-2-amine (**5**) was obtained as a white solid in 53% yield.  $^1\text{H}$  NMR (DMSO- $d_6$ , 600 MHz)  $\delta$  3.73 (s, 3H,  $\text{OCH}_3$ ), 3.77 (s, 3H,  $\text{OCH}_3$ ), 4.01 (s, 2H,  $\text{CH}_2$ ), 4.36 (d,  $J = 6.0$  Hz, 2H,  $\text{CH}_2$ ), 6.88 (t,  $J = 7.2$  Hz, 1H, ArH), 6.90–6.92 (m, 2H, ArH), 6.95 (d,  $J = 7.8$  Hz, 1H, ArH), 7.17–7.20 (m, 4H, ArH), 7.26–7.29 (m, 3H, ArH), 7.43–7.45 (m, 2H, ArH), 7.92 (t,  $J = 5.4$  Hz, 1H, NH);  $^{13}\text{C}$  NMR (151 MHz,  $\text{CDCl}_3$ )  $\delta$  167.24, 158.95, 157.46, 140.68, 129.64, 129.28, 128.85, 128.53, 128.20, 127.95, 126.41, 125.95, 120.42, 118.48, 113.67, 110.20, 55.23, 45.84, 32.95; ESI-MS  $m/z$  417  $[\text{M}+\text{H}]^+$ .

5-benzyl-N-(3-methoxybenzyl)-4-(4-methoxyphenyl)thiazol-2-amine (**6**) was obtained as a white solid in 50% yield.  $^1\text{H}$  NMR (DMSO- $d_6$ , 600 MHz)  $\delta$  3.70 (s, 3H,  $\text{OCH}_3$ ), 3.73 (s, 3H,  $\text{OCH}_3$ ), 4.02 (s, 2H,  $\text{CH}_2$ ), 4.36 (d,  $J = 6.0$  Hz, 2H,  $\text{CH}_2$ ), 6.76–6.79 (m, 1H, ArH), 6.89–6.93 (m, 4H, ArH), 7.17–7.21 (m, 4H, ArH), 7.27 (t,  $J = 7.2$ , 2H, ArH), 7.44–7.47 (m, 2H, ArH), 7.89 (t,  $J = 6.0$  Hz, 1H, NH);  $^{13}\text{C}$  NMR (151 MHz,  $\text{CDCl}_3$ )  $\delta$  167.61, 159.81, 159.03, 146.91, 140.57, 139.56, 129.62, 128.56, 128.17, 127.69, 126.67, 129.56, 119.67, 118.43, 113.71, 113.07, 112.76, 55.22, 55.18, 49.66, 32.88; ESI-MS  $m/z$  417  $[\text{M}+\text{H}]^+$ .

5-benzyl-N-(4-methoxybenzyl)-4-(4-methoxyphenyl)thiazol-2-amine (**7**) was obtained as a white solid in 85% yield, m.p. 151.2–152.4 °C.  $^1\text{H}$  NMR ( $\text{CDCl}_3$ , 300 MHz)  $\delta$  3.80 (s, 3H,  $\text{OCH}_3$ ), 3.81 (s, 3H,  $\text{OCH}_3$ ), 4.00 (d, 2H,  $J = 6.0$  Hz,  $\text{ArCH}_2$ ), 4.35 (s, 2H,  $\text{ArCH}_2$ ), 5.35 (br, 1H, NH), 6.85–6.91 (m, 4H, ArH), 7.21–7.33 (m, 7H, ArH), 7.49–7.52 (m, 2H, ArH);  $^{13}\text{C}$  NMR (151 MHz,  $\text{CDCl}_3$ )  $\delta$  167.31, 167.22, 159.01, 147.03, 140.62, 129.90, 129.67, 128.84, 128.83, 128.56, 128.17, 127.83, 126.45, 118.49, 118.43, 113.96, 113.71, 55.26, 55.24, 49.19, 32.90; ESI-MS  $m/z$  417  $[\text{M}+\text{H}]^+$ .

4-((5-benzyl-4-(4-methoxyphenyl)thiazol-2-ylamino)methyl)phenol (**8**) was obtained as a yellow solid in 96% yield, m.p. 202–203 °C.  $^1\text{H}$  NMR (DMSO- $d_6$ , 600 MHz)  $\delta$  3.76 (s, 3H,  $\text{OCH}_3$ ), 4.04 (s, 2H,  $\text{ArCH}_2$ ), 4.28 (d,  $J = 5.4$  Hz, 2H,  $\text{ArCH}_2$ ), 6.70 (d,  $J = 7.8$  Hz, 2H, ArH), 6.94 (d,  $J = 8.4$  Hz, 2H, ArH), 7.16–7.20 (m, 5H, ArH), 7.30 (t,  $J = 7.2$  Hz, 2H, ArH), 7.48 (d,  $J = 8.4$  Hz, 2H, ArH), 7.80 (br, 1H, NH), 9.29 (s, 1H, OH);  $^{13}\text{C}$  NMR (151 MHz,  $\text{CDCl}_3$ )  $\delta$  167.69, 159.28, 156.21, 140.23, 129.69, 129.26, 128.66, 128.19, 128.06, 126.64, 118.70, 116.02, 113.91, 55.25, 49.83, 32.89; ESI-MS  $m/z$  403  $[\text{M}+\text{H}]^+$ .

5-benzyl-N-(4-(dimethylamino)benzyl)-4-(4-methoxyphenyl)thiazol-2-amine (**9**) was obtained as a yellow solid in 89% yield.  $^1\text{H}$  NMR (DMSO- $d_6$ , 600 MHz)  $\delta$  2.85 (s, 6H,  $\text{CH}_3$ ), 3.76 (s, 3H,  $\text{OCH}_3$ ), 4.04 (s, 2H,  $\text{ArCH}_2$ ), 4.27 (d,  $J = 6.0$  Hz, 2H,  $\text{ArCH}_2$ ), 6.67 (d,  $J = 9.0$  Hz, 2H, ArH), 6.94 (d,  $J = 8.4$  Hz, 2H, ArH), 7.19–7.23 (m, 5H, ArH), 7.30 (t,  $J = 7.2$  Hz, 2H, ArH), 7.50 (d,  $J = 9.0$  Hz, 2H, ArH), 7.78 (t,  $J = 6.0$  Hz, 1H, NH);  $^{13}\text{C}$  NMR (151 MHz,  $\text{CDCl}_3$ )  $\delta$  167.24, 167.17, 158.98, 150.13, 147.13, 140.71, 129.68, 128.74, 128.56, 128.20, 127.98, 126.42, 125.41, 118.39, 118.35, 113.71, 112.61, 55.25, 49.41, 40.63, 40.62, 32.94; ESI-MS  $m/z$  430  $[\text{M}+\text{H}]^+$ .

5-benzyl-N-(4-fluorobenzyl)-4-(4-methoxyphenyl)thiazol-2-amine (**10**) was obtained as a white solid in 62% yield, m.p. 123.4–123.8 °C.  $^1\text{H}$  NMR ( $\text{CDCl}_3$ , 600 MHz)  $\delta$  3.81 (s, 3H,  $\text{OCH}_3$ ), 4.10 (s, 2H,  $\text{ArCH}_2$ ), 4.39 (s, 2H,  $\text{ArCH}_2$ ), 5.80 (br, 1H, NH), 6.90 (d,  $J = 8.4$  Hz, 2H, ArH), 7.02 (d,  $J = 8.4$  Hz, 2H, ArH), 7.23–7.33 (m, 7H, ArH), 7.50 (d,  $J = 7.5$  Hz, 2H, ArH);  $^{13}\text{C}$  NMR (151 MHz,  $\text{CDCl}_3$ )  $\delta$  167.02, 163.01, 161.38, 159.11, 140.35, 133.37, 129.65, 129.24, 129.18, 128.60, 128.43, 128.15, 126.55, 118.68, 115.54, 115.40, 113.75, 55.25, 49.01, 32.86; ESI-MS  $m/z$  477  $[\text{M}+\text{H}]^+$ .

5-benzyl-4-(4-methoxyphenyl)-N-(4-nitrobenzyl)thiazol-2-amine (**11**) was obtained as a slightly yellow solid in 65% yield, m.p. 161.9–163.4 °C.  $^1\text{H}$  NMR ( $\text{CDCl}_3$ , 600 MHz)  $\delta$  3.80 (s, 3H,  $\text{OCH}_3$ ), 4.07 (s, 2H,  $\text{ArCH}_2$ ), 4.53 (s, 2H,  $\text{ArCH}_2$ ), 6.50 (br, 1H, NH), 6.88 (d,  $J = 8.4$  Hz, 2H, ArH), 7.19 (d,  $J = 7.2$  Hz, 2H, ArH), 7.23–7.48 (m, 5H,

ArH), 7.50 (d,  $J = 8.4$  Hz, 2H, ArH), 7.50 (d,  $J = 7.2$  Hz, 2H, ArH);  $^{13}\text{C}$  NMR (151 MHz,  $\text{CDCl}_3$ )  $\delta$  167.80, 159.17, 147.18, 145.75, 140.26, 129.66, 128.62, 128.10, 127.75, 126.60, 123.67, 118.86, 113.71, 55.20, 48.93, 32.79; ESI-MS  $m/z$  432  $[\text{M}+\text{H}]^+$ .

5-benzyl-4-(4-methoxyphenyl)-N-(3-nitrobenzyl)thiazol-2-amine (**12**) was obtained as a yellow solid in 91% yield, m.p. 151–152 °C.  $^1\text{H}$  NMR ( $\text{CDCl}_3$ , 600 MHz)  $\delta$  3.80 (s, 3H,  $\text{OCH}_3$ ), 4.08 (s, 2H,  $\text{ArCH}_2$ ), 4.55 (s, 2H,  $\text{ArCH}_2$ ), 5.75 (br, 1H, NH), 6.88 (d,  $J = 8.4$  Hz, 2H, ArH), 7.24–7.18 (m, 3H, ArH) 7.31 (t,  $J = 7.4$  Hz, 2H, ArH), 7.51 (dd,  $J_1 = 19.9$  Hz,  $J_2 = 8.1$  Hz, 3H, ArH), 7.71 (d,  $J = 7.2$  Hz, 1H, ArH), 8.14 (d,  $J = 8.2$  Hz, 1H, ArH), 8.24 (s, 1H, NH);  $^{13}\text{C}$  NMR (151 MHz,  $\text{CDCl}_3$ )  $\delta$  133.61, 129.65, 129.60, 128.63, 128.18, 126.58, 122.63, 122.55, 113.80, 97.50, 55.07, 48.79, 30.93; ESI-MS  $m/z$  432  $[\text{M}+\text{H}]^+$ .

4-((5-benzyl-4-(4-methoxyphenyl)thiazol-2-ylamino)methyl)benzonitrile (**13**) was obtained as a yellow solid in 73% yield, m.p. 164–165 °C.  $^1\text{H}$  NMR (DMSO- $d_6$ , 600 MHz)  $\delta$  3.75 (s, 3H,  $\text{OCH}_3$ ), 4.05 (s, 2H,  $\text{ArCH}_2$ ), 4.52 (d,  $J = 6.0$  Hz, 2H,  $\text{ArCH}_2$ ), 6.93 (d,  $J = 8.4$  Hz, 2H, ArH), 7.24–7.19 (m, 3H, ArH), 7.30 (t,  $J = 7.8$  Hz, 2H, ArH), 7.46 (d,  $J = 8.4$  Hz, 2H, ArH), 7.56 (d,  $J = 7.2$  Hz, 2H, ArH), 7.80 (d,  $J = 7.8$  Hz, 2H, ArH), 8.04 (t,  $J = 5.4$  Hz, 1H, NH);  $^{13}\text{C}$  NMR (151 MHz,  $\text{CDCl}_3$ )  $\delta$  167.63, 159.21, 143.52, 140.18, 132.30, 132.15, 129.66, 128.63, 128.11, 127.77, 127.01, 126.62, 118.80, 118.74, 113.75, 111.14, 55.23, 49.14, 32.79; ESI-MS  $m/z$  412  $[\text{M}+\text{H}]^+$ .

5-benzyl-N-(2,6-dichlorobenzyl)-4-(4-methoxyphenyl)thiazol-2-amine (**14**) was obtained as a slightly yellow solid in 18.5% yield, m.p. 171–172 °C.  $^1\text{H}$  NMR (DMSO- $d_6$ , 600 MHz)  $\delta$  3.77 (s, 3H,  $\text{OCH}_3$ ), 4.07 (s, 2H,  $\text{CH}_2$ ), 4.66 (d, 2H,  $J = 4.2$ ,  $\text{CH}_2$ ), 6.96 (d, 2H,  $J = 8.4$ , ArH), 7.25–7.18 (m, 3H, ArH), 7.31 (t, 2H,  $J = 7.8$ , ArH), 7.38 (t, 1H,  $J = 8.4$ , ArH), 7.58–7.50 (m, 4H, ArH), 7.66 (s, 1H, NH);  $^{13}\text{C}$  NMR (151 MHz,  $\text{CDCl}_3$ )  $\delta$  164.86, 159.05, 146.90, 140.40, 129.59, 128.58, 128.15, 126.53, 113.75, 55.26, 32.89.

2-((5-benzyl-4-(4-methoxyphenyl)thiazol-2-ylamino)methyl)-4-nitrophenol (**15**) was obtained as a yellow solid in 53.8% yield, m.p. 182–183 °C.  $^1\text{H}$  NMR ( $\text{CDCl}_3$ , 600 MHz)  $\delta$  3.86 (s, 3H,  $\text{OCH}_3$ ), 4.06 (s, 2H,  $\text{CH}_2$ ), 4.55 (s, 2H,  $\text{CH}_2$ ), 5.55 (br, 1H, NH), 6.95 (d, 1H,  $J = 6.0$  Hz, ArH), 6.99 (d, 2H,  $J = 12.0$  Hz, ArH), 7.19 (d, 2H,  $J = 6.0$  Hz, ArH), 7.23–7.25 (t, 1H,  $J = 6.0$  Hz, ArH), 7.29–7.31 (t, 2H,  $J = 6.0$  Hz, ArH), 7.53 (d, 2H,  $J = 12.0$  Hz, ArH), 8.08–8.12 (dd, 2H,  $J_1 = 3.0$  Hz,  $J_2 = 3.0$  Hz, ArH), 12.79 (s, 1H, OH);  $^{13}\text{C}$  NMR (151 MHz,  $\text{CDCl}_3$ )  $\delta$  167.13, 163.32, 159.66, 129.63, 128.71, 128.14, 127.49, 126.80, 125.92, 114.08, 55.29, 44.96, 32.85; HRMS calculated for  $\text{C}_{24}\text{H}_{21}\text{N}_3\text{O}_4\text{S}$  ( $\text{M}+\text{H})^+$  448.1331; found 448.1458; IR (KBr,  $\text{cm}^{-1}$ ): 3401 ( $\nu_{\text{O-H}}$ ), 3327 ( $\nu_{\text{N-H}}$ ), 3050 ( $\nu_{\text{Ar-H}}$ ), 3032 ( $\nu_{\text{Ar-H}}$ ), 2937, 2831, 1612, 1582, 1544, 1511, 1336, 1290, 1251, 1171, 1093, 1032, 836, 751, 702.

4-((5-benzyl-4-(4-methoxyphenyl)thiazol-2-ylamino)methyl)-2-methoxyphenol (**16**) was obtained as a white solid in 73% yield, m.p. 137–138 °C.  $^1\text{H}$  NMR ( $\text{CDCl}_3$ , 600 MHz)  $\delta$  3.73 (s, 3H,  $\text{OCH}_3$ ), 3.76 (s, 3H,  $\text{OCH}_3$ ), 4.10 (s, 2H,  $\text{ArCH}_2$ ), 4.28 (d,  $J = 5.7$  Hz, 2H,  $\text{ArCH}_2$ ), 6.71 (d,  $J = 8.0$  Hz, 1H, ArH), 6.75 (dd,  $J_1 = 8.0$  Hz,  $J_2 = 1.9$  Hz, 1H, ArH), 6.97–6.93 (m, 3H, ArH), 7.24–7.16 (m, 3H, ArH), 7.30 (t,  $J = 7.6$  Hz, 2H, ArH), 7.53–7.47 (m, 2H, ArH), 7.78 (t,  $J = 5.8$  Hz, 1H, NH), 8.83 (s, 1H, OH);  $^{13}\text{C}$  NMR (151 MHz,  $\text{CDCl}_3$ )  $\delta$  167.03, 159.35, 146.72, 145.23, 140.28, 129.66, 128.60, 128.16, 126.57, 120.76, 118.74, 114.30, 113.80, 110.28, 55.93, 55.25, 49.84, 32.87; ESI-MS  $m/z$  433  $[\text{M}+\text{H}]^+$ .

5-benzyl-4-(4-methoxyphenyl)-N-(3,4,5-trimethoxybenzyl)thiazol-2-amine (**17**) was obtained as a white solid in 72.5% yield.  $^1\text{H}$  NMR ( $\text{CDCl}_3$ , 600 MHz)  $\delta$  3.82 (3H, s,  $\text{OCH}_3$ ), 3.83 (9H, s,  $3 \times \text{OCH}_3$ ), 4.10 (2H, s,  $\text{ArCH}_2$ ), 4.34 (2H, s,  $\text{ArCH}_2\text{NH}$ ), 5.93 (1H, br, NH), 6.57 (2H, s, ArH), 6.91 (2H, d,  $J = 8.4$  Hz, ArH), 7.23–7.32 (5H, m, ArH), 7.51 (2H, d,  $J = 8.4$  Hz, ArH).  $^{13}\text{C}$  NMR (151 MHz,  $\text{CDCl}_3$ )  $\delta$  167.68, 159.02, 153.24, 146.93, 140.55, 137.08, 133.66, 129.59, 128.56, 128.14, 127.69, 126.50, 118.55, 113.70, 104.26, 60.79, 55.98, 55.21, 49.95, 32.90; m.p. 126.5–128.3 °C.

5-benzyl-N-(furan-2-ylmethyl)-4-(4-methoxyphenyl)thiazol-2-amine (**18**) was obtained as a white solid in 94% yield, m.p.

126–127 °C.  $^1\text{H}$  NMR ( $\text{CDCl}_3$ , 600 MHz)  $\delta$  3.81 (s, 3H,  $\text{OCH}_3$ ), 4.10 (s, 2H,  $\text{ArCH}_2$ ), 4.41 (s, 2H,  $\text{ArCH}_2$ ), 5.46 (s, 1H, NH), 6.27 (d,  $J = 3.2$  Hz, 1H, ArH), 6.32 (t,  $J = 2.5$  Hz, 1H, ArH), 6.95–6.86 (m, 2H, ArH), 7.23 (d,  $J = 14.1$  Hz, 3H, ArH), 7.31 (t,  $J = 7.6$  Hz, 2H, ArH), 7.38–7.35 (m, 1H, ArH), 7.53–7.49 (m, 2H, ArH);  $^{13}\text{C}$  NMR (151 MHz,  $\text{CDCl}_3$ )  $\delta$  166.74, 159.05, 151.23, 147.03, 142.17, 140.55, 129.70, 128.57, 128.18, 127.77, 126.48, 118.91, 113.73, 110.36, 107.66, 55.26, 42.59, 32.89; ESI-MS  $m/z$  377  $[\text{M}+\text{H}]^+$ .

*5-benzyl-4-(4-methoxyphenyl)-N-(pyridin-3-ylmethyl)thiazol-2-amine (19)* was obtained as a yellow solid in 75% yield, m.p. 145–146 °C.  $^1\text{H}$  NMR ( $\text{CDCl}_3$ , 600 MHz)  $\delta$  3.80 (s, 3H,  $\text{OCH}_3$ ), 4.08 (s, 2H,  $\text{ArCH}_2$ ), 4.42 (s, 2H,  $\text{ArCH}_2$ ), 6.01 (br, 1H, NH), 6.95–6.82 (m, 2H, ArH), 7.28–7.19 (m, 4H, ArH), 7.30 (t,  $J = 7.5$  Hz, 2H, ArH), 7.51–7.46 (m, 2H, ArH), 7.73–7.70 (m, 1H, ArH), 8.53 (dd,  $J_1 = 4.7$  Hz,  $J_2 = 1.6$  Hz, 1H, ArH), 8.62–8.56 (m, 1H, ArH);  $^{13}\text{C}$  NMR (151 MHz,  $\text{CDCl}_3$ )  $\delta$  167.28, 159.14, 149.02, 148.79, 140.31, 135.15, 133.54, 129.67, 128.59, 128.13, 126.54, 123.45, 118.74, 113.75, 55.23, 47.01, 32.82; ESI-MS  $m/z$  388  $[\text{M}+\text{H}]^+$ .

*5-benzyl-4-(4-methoxyphenyl)-N-(naphthalen-2-ylmethyl)thiazol-2-amine (20)* was obtained as a yellow solid in 73% yield, m.p. 145–146 °C.  $^1\text{H}$  NMR ( $\text{CDCl}_3$ , 600 MHz)  $\delta$  3.80 (s, 3H,  $\text{OCH}_3$ ), 4.08 (s, 2H,  $\text{ArCH}_2$ ), 4.42 (s, 2H,  $\text{ArCH}_2$ ), 6.01 (br, 1H, NH), 6.92–6.84 (m, 2H, ArH), 7.24–7.20 (m, 3H, ArH), 7.29 (t,  $J = 7.6$  Hz, 2H, ArH), 7.56–7.43 (m, 5H, ArH), 7.87–7.74 (m, 4H, ArH);  $^{13}\text{C}$  NMR (151 MHz,  $\text{CDCl}_3$ )  $\delta$  167.56, 159.08, 140.44, 135.15, 133.30, 132.82, 129.69, 128.58, 128.41, 128.16, 127.82, 127.67, 126.49, 126.19, 126.10, 125.87, 125.54, 118.54, 113.74, 55.21, 49.92, 32.86; ESI-MS  $m/z$  388  $[\text{M}+\text{H}]^+$ .

*5-benzyl-4-(2-fluorophenyl)-N-(4-methoxybenzyl)thiazol-2-amine (21)* was obtained as a white solid in 43% yield.  $^1\text{H}$  NMR ( $\text{DMSO}-d_6$ , 600 MHz)  $\delta$  3.72 (s, 3H,  $\text{OCH}_3$ ), 3.81 (s, 2H,  $\text{CH}_2$ ), 4.30 (d,  $J = 5.4$  Hz, 2H,  $\text{CH}_2$ ), 6.89–6.85 (m, 2H, ArH), 7.10 (d,  $J = 7.8$  Hz, 2H, ArH), 7.17 (t,  $J = 7.2$  Hz, 1H, ArH), 7.21–7.31 (m, 6H, ArH), 7.45–7.41 (m, 2H, ArH), 7.89 (t,  $J = 5.4$  Hz, 1H, NH);  $^{13}\text{C}$  NMR (151 MHz,  $\text{CDCl}_3$ )  $\delta$  167.28, 160.66, 159.07, 141.45, 140.40, 131.79, 129.63, 128.95, 128.38 (d,  $J = 17.0$  Hz), 126.45, 124.03, 123.27, 123.18, 115.98, 115.83, 114.03, 55.26, 49.25, 33.07, 33.05; ESI-MS  $m/z$  405  $[\text{M}+\text{H}]^+$ .

*5-benzyl-4-(4-fluorophenyl)-N-(4-methoxybenzyl)thiazol-2-amine (22)* was obtained as a yellow solid in 93% yield, m.p. 139–140 °C.  $^1\text{H}$  NMR ( $\text{DMSO}-d_6$ , 600 MHz)  $\delta$  3.73 (s, 3H,  $\text{OCH}_3$ ), 4.05 (s, 2H,  $\text{ArCH}_2$ ), 4.34 (d,  $J = 5.4$  Hz, 2H,  $\text{ArCH}_2$ ), 6.86 (d,  $J = 9.0$  Hz, 2H, ArH), 7.18 (d,  $J = 7.2$  Hz, 2H, ArH), 7.24–7.20 (m, 3H, ArH), 7.34–7.28 (m, 4H, ArH), 7.62–7.57 (m, 2H, ArH), 7.93 (br, 1H, NH);  $^{13}\text{C}$  NMR (151 MHz,  $\text{CDCl}_3$ )  $\delta$  166.94, 163.00, 161.36, 159.12, 146.54, 140.32, 131.41, 130.12, 129.71, 128.90, 128.61, 128.11, 126.55, 119.73, 115.27, 115.12, 114.03, 55.27, 49.20, 32.84, 30.90; ESI-MS  $m/z$  405  $[\text{M}+\text{H}]^+$ .

*5-benzyl-4-(2,4-difluorophenyl)-N-(4-methoxybenzyl)thiazol-2-amine (23)* was obtained as a slightly yellow solid in 62% yield.  $^1\text{H}$  NMR ( $\text{DMSO}-d_6$ , 600 MHz)  $\delta$  3.69 (s, 3H,  $\text{OCH}_3$ ), 3.78 (s, 2H,  $\text{CH}_2$ ), 4.27 (d,  $J = 5.0$  Hz, 2H,  $\text{CH}_2$ ), 6.85 (d,  $J = 8.4$  Hz, 2H, ArH), 7.08 (d,  $J = 7.2$  Hz, 2H, ArH), 7.16–7.12 (m, 2H, ArH), 7.27–7.20 (m, 4H, ArH), 7.28 (td,  $J_1 = 10.2$  Hz,  $J_2 = 2.4$  Hz, 1H, ArH), 7.47 (dd,  $J_1 = 15.6$  Hz,  $J_2 = 8.4$  Hz, 1H, ArH), 7.89 (t,  $J = 6.0$  Hz, 1H, NH).  $^{13}\text{C}$  NMR (151 MHz,  $\text{CDCl}_3$ )  $\delta$  167.70, 163.53, 161.91, 160.85, 159.08, 140.45, 140.20, 132.59, 129.62, 128.78, 128.49, 128.28, 126.52, 123.02, 114.00, 111.33, 104.34, 104.17, 104.00, 55.26, 49.16, 32.97; ESI-MS  $m/z$  423  $[\text{M}+\text{H}]^+$ .

*5-benzyl-4-(2-chlorophenyl)-N-(4-methoxybenzyl)thiazol-2-amine (24)* was obtained as a yellow solid in 86% yield.  $^1\text{H}$  NMR ( $\text{DMSO}-d_6$ , 600 MHz)  $\delta$  3.69 (s, 3H,  $\text{OCH}_3$ ), 3.71 (s, 2H,  $\text{CH}_2$ ), 4.26 (d,  $J = 5.4$  Hz, 2H,  $\text{CH}_2$ ), 6.85 (d,  $J = 8.4$  Hz, 2H, ArH), 7.06 (d,  $J = 7.2$  Hz, 2H, ArH), 7.14 (t,  $J = 7.2$  Hz, 1H, ArH), 7.23 (dd,  $J_1 = 9.0$  Hz,  $J_2 = 7.8$  Hz, 4H, ArH), 7.39–7.33 (m, 3H, ArH), 7.51 (d,  $J = 7.8$  Hz, 1H, ArH), 7.84 (t,  $J = 5.4$  Hz, 1H, NH).  $^{13}\text{C}$  NMR (151 MHz,  $\text{CDCl}_3$ )  $\delta$  167.89, 158.94, 144.67, 140.36, 134.58, 134.10, 131.96, 129.85, 129.72, 129.37, 128.81, 128.58, 128.43, 128.30, 126.54, 126.41, 122.07, 113.89, 55.26, 49.06, 32.95; ESI-MS  $m/z$  421  $[\text{M}+\text{H}]^+$ .

*5-benzyl-4-(2,4-dichlorophenyl)-N-(4-methoxybenzyl)thiazol-2-amine (25)* was obtained as a slightly yellow solid in 69% yield.  $^1\text{H}$  NMR ( $\text{DMSO}-d_6$ , 600 MHz)  $\delta$  3.73 (s, 3H,  $\text{OCH}_3$ ), 3.75 (s, 2H,  $\text{CH}_2$ ), 4.30 (d,  $J = 5.4$  Hz, 2H,  $\text{CH}_2$ ), 6.88 (d,  $J = 7.8$  Hz, 2H, ArH), 7.10 (d,  $J = 7.2$  Hz, 2H, ArH), 7.18 (t,  $J = 7.2$  Hz, 1H, ArH), 7.26 (dd,  $J_1 = 10.8$  Hz,  $J_2 = 8.4$  Hz, 4H, ArH), 7.43 (d,  $J = 8.4$  Hz, 1H, ArH), 7.49–7.46 (m, 1H, ArH), 7.73–7.70 (m, 1H, ArH), 7.92 (t,  $J = 5.4$  Hz, 1H, NH);  $^{13}\text{C}$  NMR (151 MHz,  $\text{CDCl}_3$ )  $\delta$  168.05, 167.99, 158.98, 143.49, 140.07, 134.85, 134.49, 133.12, 132.66, 129.66, 129.53, 128.61, 128.58, 128.49, 128.24, 126.88, 126.52, 122.49, 113.92, 55.27, 49.13, 32.91; ESI-MS  $m/z$  455  $[\text{M}+\text{H}]^+$ .

*5-benzyl-4-(2,5-dimethoxyphenyl)-N-(4-methoxybenzyl)thiazol-2-amine (26)* was obtained as a white solid in 65.1% yield, m.p. 162.3–163.8 °C.  $^1\text{H}$  NMR ( $\text{CDCl}_3$ , 600 MHz)  $\delta$  3.65 (s, 3H,  $\text{OCH}_3$ ), 3.69 (s, 3H,  $\text{OCH}_3$ ), 3.72 (s, 3H,  $\text{OCH}_3$ ), 3.73 (s, 2H,  $\text{ArCH}_2$ ), 4.28 (d, 2H,  $J = 5.8$  Hz,  $\text{ArCH}_2$ ), 6.83 (d,  $J = 3.2$  Hz, 1H, ArH), 6.92–6.86 (m, 3H), 6.99 (d,  $J = 9.0$  Hz, 1H, ArH), 7.11 (dd,  $J_1 = 7.9$  Hz,  $J_2 = 1.4$  Hz, 2H, ArH), 7.16 (td,  $J_1 = 7.2$  Hz,  $J_2 = 1.3$  Hz, 1H, ArH), 7.28–7.23 (m, 4H, ArH), 7.78 (t,  $J = 5.8$  Hz, 1H, NH);  $^{13}\text{C}$  NMR (151 MHz,  $\text{CDCl}_3$ )  $\delta$  167.25, 159.02, 153.36, 151.36, 143.82, 140.90, 129.91, 128.93, 128.37, 128.30, 126.21, 125.24, 122.03, 116.72, 114.71, 113.94, 112.51, 56.13, 55.70, 55.25, 49.24, 33.16; ESI-MS  $m/z$  447  $[\text{M}+\text{H}]^+$ .

*5-benzyl-4-(furan-2-yl)-N-(4-methoxybenzyl)thiazol-2-amine (27)* was obtained as a white solid in 95% yield.  $^1\text{H}$  NMR ( $\text{CDCl}_3$ , 300 MHz)  $\delta$  3.72 (s, 3H,  $\text{OCH}_3$ ), 4.23 (s, 2H,  $\text{ArCH}_2$ ), 4.32 (d,  $J = 5.4$  Hz, 2H,  $\text{ArCH}_2$ ), 6.55–6.53 (m, 1H, ArH), 6.60 (d,  $J = 3.0$  Hz, 1H, ArH), 6.88 (d,  $J = 8.4$  Hz, 2H, ArH), 7.24–7.19 (m, 3H, ArH), 7.32–7.26 (m, 4H, ArH), 7.70 (s, 1H, ArH), 7.94 (br, 1H, NH);  $^{13}\text{C}$  NMR (151 MHz,  $\text{CDCl}_3$ )  $\delta$  167.27, 159.10, 150.52, 141.54, 140.31, 137.52, 129.61, 128.88, 128.54, 128.33, 126.48, 120.74, 114.02, 111.10, 107.94, 55.25, 49.28, 32.61; ESI-MS  $m/z$  377  $[\text{M}+\text{H}]^+$ .

*5-benzyl-N-(4-methoxybenzyl)-4-phenylthiazol-2-amine (28)* was obtained as a white solid in 91% yield, m.p. 114–115 °C.  $^1\text{H}$  NMR ( $\text{DMSO}-d_6$ , 600 MHz)  $\delta$  3.71 (s, 3H,  $\text{OCH}_3$ ), 4.05 (s, 2H,  $\text{ArCH}_2$ ), 4.33 (d,  $J = 3.0$  Hz, 2H,  $\text{ArCH}_2$ ), 6.87–6.83 (m, 2H, ArH), 7.16 (d,  $J = 7.2$  Hz, 2H, ArH), 7.21–7.19 (m, 1H, ArH), 7.34–7.24 (m, 5H, ArH), 7.38 (t,  $J = 7.8$  Hz, 2H, ArH), 7.54 (d,  $J = 7.8$  Hz, 2H, ArH), 7.87 (t,  $J = 5.4$  Hz, 1H, NH);  $^{13}\text{C}$  NMR (151 MHz,  $\text{CDCl}_3$ )  $\delta$  166.95, 159.08, 159.04, 158.23, 132.56, 129.65, 129.14, 128.93, 119.29, 114.00, 113.95, 113.73, 55.26, 55.24, 49.29, 32.07.

*5-(2-methoxybenzyl)-N-(4-methoxybenzyl)-4-phenylthiazol-2-amine (29)* was obtained as a white solid in 96.3% yield, m.p. 144.7–145.2 °C.  $^1\text{H}$  NMR ( $\text{DMSO}-d_6$ , 600 MHz)  $\delta$  3.77 (s, 3H,  $\text{OCH}_3$ ), 3.78 (s, 3H,  $\text{OCH}_3$ ), 4.03 (s, 2H,  $\text{ArCH}_2$ ), 4.39 (d, 2H,  $\text{ArCH}_2$ ), 6.92 (t,  $J = 9.00$  Hz, 1H, ArH), 6.94 (d,  $J = 9.00$  Hz, 2H, ArH), 7.03 (d,  $J = 9.00$  Hz, 1H, ArH), 7.11 (d,  $J = 6.60$  Hz, 1H, ArH), 7.27 (t,  $J = 7.80$  Hz, 1H, ArH), 7.34 (d,  $J = 9.00$  Hz, 2H, ArH), 7.35 (t,  $J = 6.60$  Hz, 1H, ArH), 7.43 (t,  $J = 7.80$  Hz, 2H, ArH), 7.60 (d,  $J = 7.80$  Hz, 2H, ArH), 7.98 (t, 1H, NH);  $^{13}\text{C}$  NMR (151 MHz,  $\text{CDCl}_3$ )  $\delta$  167.12, 159.02, 156.98, 147.27, 135.53, 129.98, 129.35, 128.93, 128.51, 128.20, 127.70, 127.31, 120.55, 119.64, 113.96, 110.11, 55.26, 55.16, 49.20, 27.23; ESI-MS  $m/z$  417  $[\text{M}+\text{H}]^+$ ; IR (KBr,  $\text{cm}^{-1}$ ): 3204 ( $\nu_{\text{N-H}}$ ), 3099, 2954, 2831, 1582, 1510, 1491, 1460, 1172, 1034, 824, 763, 701.

*4-((2-(4-methoxybenzylamino)-4-phenylthiazol-5-yl)methyl)benzotriazole (30)* was obtained as a white solid in 96% yield, m.p. 138.1–138.9 °C.  $^1\text{H}$  NMR ( $\text{DMSO}-d_6$ , 600 MHz)  $\delta$  3.72 (s, 3H,  $\text{OCH}_3$ ), 4.17 (s, 2H,  $\text{ArCH}_2$ ), 4.34 (d, 2H,  $\text{ArCH}_2$ ), 6.89 (d,  $J = 8.40$  Hz, 2H, ArH), 7.28 (d,  $J = 8.40$  Hz, 2H, ArH), 7.30 (t, 1H, ArH), 7.36–7.39 (m, 4H, ArH), 7.52 (d,  $J = 7.80$  Hz, 2H, ArH), 7.77 (d,  $J = 7.8$  Hz, 2H, ArH), 7.98 (br, 1H, NH);  $^{13}\text{C}$  NMR (151 MHz,  $\text{CDCl}_3$ )  $\delta$  167.31, 159.15, 145.94, 132.41, 129.46, 128.90, 128.45, 128.37, 127.86, 118.83, 117.35, 114.04, 110.46, 55.27, 49.21, 32.91; ESI-MS  $m/z$  412  $[\text{M}+\text{H}]^+$ ; IR (KBr,  $\text{cm}^{-1}$ ): 3205 ( $\nu_{\text{N-H}}$ ), 3094, 2972, 2910, 2227, 1586, 1513, 1460, 1434, 1176, 1036, 813, 698.

*N-(4-methoxybenzyl)-4-(4-methoxyphenyl)-5-methylthiazol-2-amine (31)* was obtained as a white solid in 79% yield, m.p.

123–124 °C. <sup>1</sup>H NMR (DMSO-*d*<sub>6</sub>, 600 MHz) δ 2.28 (s, 3H, CH<sub>3</sub>), 3.72 (s, 3H, OCH<sub>3</sub>), 3.77 (s, 3H, OCH<sub>3</sub>), 4.33 (d, *J* = 6.0 Hz, 2H, ArCH<sub>2</sub>), 6.88 (d, *J* = 9.0 Hz, 2H, ArH), 6.96 (d, *J* = 8.4 Hz, 2H, ArH), 7.28 (d, *J* = 7.8 Hz, 2H, ArH), 7.50 (d, *J* = 8.4 Hz, 2H, ArH), 7.81 (br, 1H, NH); <sup>13</sup>C NMR (151 MHz, CDCl<sub>3</sub>) δ 166.20, 159.15, 159.01, 132.80, 129.62, 129.43, 129.15, 128.98, 128.84, 114.35, 114.19, 114.03, 113.75, 55.57, 55.25, 49.34, 26.47, 12.34; ESI-MS *m/z* 341[M+H]<sup>+</sup>. The purity of this compound is 92.54%.

*N*-(4-methoxybenzyl)-4-(4-methoxyphenyl)-5-(4-nitrobenzyl)thiazol-2-amine (**32**) was obtained as a yellow solid in 69% yield, m.p. 168–169 °C. <sup>1</sup>H NMR (DMSO-*d*<sub>6</sub>, 600 MHz) δ 3.72 (s, 3H, OCH<sub>3</sub>), 3.75 (s, 3H, OCH<sub>3</sub>), 4.20 (s, 2H, ArCH<sub>2</sub>), 4.34 (d, *J* = 5.4 Hz, 2H, ArCH<sub>2</sub>), 6.89–6.85 (m, 2H, ArH), 6.96 (d, *J* = 7.2 Hz, 2H, ArH), 7.24 (d, *J* = 3.0 Hz, 2H, ArH), 7.42 (d, *J* = 3.0 Hz, 4H, ArH), 7.94 (t, 1H, NH), 8.18 (d, *J* = 9.0 Hz, 2H, ArH); <sup>13</sup>C NMR (151 MHz, CDCl<sub>3</sub>) δ 166.76, 159.27, 159.24, 148.51, 148.19, 146.78, 129.58, 129.54, 129.02, 128.97, 123.89, 116.30, 114.12, 113.89, 55.31, 49.28, 32.81; ESI-MS *m/z* 462[M+H]<sup>+</sup>.

5-(4-fluorobenzyl)-*N*-(4-methoxybenzyl)-4-(4-methoxyphenyl)thiazol-2-amine (**33**) was obtained as a white solid in 99% yield, m.p. 127–128 °C. <sup>1</sup>H NMR (DMSO-*d*<sub>6</sub>, 600 MHz) δ 3.72 (s, 3H, OCH<sub>3</sub>), 3.76 (s, 3H, OCH<sub>3</sub>), 4.03 (s, 2H, ArCH<sub>2</sub>), 4.33 (d, *J* = 6.0 Hz, 2H, ArCH<sub>2</sub>), 6.88 (d, *J* = 8.4 Hz, 2H, ArH), 6.96 (d, *J* = 8.4 Hz, 2H, ArH), 7.12 (t, *J* = 8.4 Hz, 2H, ArH), 7.24–7.20 (m, 2H, ArH), 7.28 (d, *J* = 8.4 Hz, 2H, ArH), 7.48 (d, *J* = 9.0 Hz, 2H, ArH), 7.86 (s, 1H, NH); <sup>13</sup>C NMR (151 MHz, CDCl<sub>3</sub>) δ 167.06, 162.40, 160.78, 159.12, 136.12, 129.63, 129.60, 129.54, 128.92, 118.30, 115.43, 115.29, 114.01, 113.77, 55.26, 55.24, 49.27, 32.10; ESI-MS *m/z* 435[M+H]<sup>+</sup>.

*N*,5-bis(4-methoxybenzyl)-4-(4-methoxyphenyl)thiazol-2-amine (**34**) was obtained as a white solid in 90% yield, m.p. 132–133 °C. <sup>1</sup>H NMR (DMSO-*d*<sub>6</sub>, 600 MHz) δ 3.70 (s, 3H, OCH<sub>3</sub>), 3.72 (s, 3H, OCH<sub>3</sub>), 3.76 (s, 3H, OCH<sub>3</sub>), 3.97 (s, 2H, ArCH<sub>2</sub>), 4.33 (d, *J* = 5.4 Hz, 2H, ArCH<sub>2</sub>), 6.89–6.81 (m, 4H, ArH), 6.96 (d, *J* = 9.0 Hz, 2H, ArH), 7.10 (d, *J* = 8.4 Hz, 2H, ArH), 7.28 (d, *J* = 8.4 Hz, 2H, ArH), 7.49 (d, *J* = 9.0 Hz, 2H, ArH), 7.87 (br, 1H, NH); <sup>13</sup>C NMR (151 MHz, CDCl<sub>3</sub>) δ 166.92, 159.10, 140.52, 135.25, 129.78, 128.95, 128.56, 128.46, 128.30, 128.18, 127.49, 126.48, 120.02, 114.02, 55.27, 49.24, 32.92.

5-benzyl-*N*-(4-methoxybenzyl)-4-(4-methoxyphenyl)-*N*-methylthiazol-2-amine (**35**) was obtained as a slightly green oil in 68% yield. <sup>1</sup>H NMR (DMSO-*d*<sub>6</sub>, 600 MHz) δ 2.93 (s, 3H, CH<sub>3</sub>), 3.72 (s, 3H, OCH<sub>3</sub>), 3.77 (s, 3H, OCH<sub>3</sub>), 4.09 (s, 2H, ArCH<sub>2</sub>), 4.56 (s, 2H, ArCH<sub>2</sub>), 6.89 (d, *J* = 8.4 Hz, 2H, ArH), 6.96 (d, *J* = 9.0 Hz, 2H, ArH), 7.20 (d, *J* = 7.8 Hz, 3H, ArH), 7.26–7.22 (m, 2H, ArH), 7.32 (t, *J* = 7.8 Hz, 2H, ArH), 7.53 (d, *J* = 9.0 Hz, 2H, ArH); <sup>13</sup>C NMR (151 MHz, CDCl<sub>3</sub>) δ 168.05, 158.99, 158.92, 147.80, 140.81, 132.83, 129.70, 129.19, 129.17, 128.79, 128.54, 128.41, 128.38, 128.22, 126.39, 118.34, 113.93, 113.68, 113.54, 113.29, 55.49, 55.27, 55.25, 37.36, 33.05, 30.91.

(*E*)-5-benzyl-*N*-(4-methoxybenzylidene)-4-phenylthiazol-2-amine (**36**) was obtained as a yellow solid in 52%, m.p. 107–108 °C. <sup>1</sup>H NMR (DMSO-*d*<sub>6</sub>, 600 MHz) δ 3.77 (s, 3H, OCH<sub>3</sub>), 4.21 (s, 2H, ArCH<sub>2</sub>), 6.99–6.96 (m, 2H, ArH), 7.16 (t, *J* = 8.6 Hz, 2H, ArH), 7.29–7.23 (m, 3H, ArH), 7.34 (dd, *J*<sub>1</sub> = 8.2 Hz, *J*<sub>2</sub> = 6.8 Hz, 2H, ArH), 7.61 (d, *J* = 8.7 Hz, 2H, ArH), 7.98–7.94 (m, 2H, ArH), 8.92 (s, 1H, N=CH); <sup>13</sup>C NMR (151 MHz, CDCl<sub>3</sub>) δ 169.14, 161.10, 159.38, 150.01, 139.97, 131.84, 131.45, 131.02, 129.97, 128.75, 128.33, 127.30, 126.80, 116.24, 116.09, 113.86, 55.30, 33.54.

5-benzyl-2-chloro-4-(4-methoxyphenyl)thiazole (**43**). Compound **42a** (10.0 g, 33.7 mmol) and 100 mL of acetonitrile were added into a 250 mL three-necked flask at 0 °C and stirred until dissolved. Then, the nitrite isoamyl acetate (5.9 g, 50.6 mmol) was added and stirred at this temperature for 20 min. Copper chloride dihydrate (6.9 g, 5.06 mmol) was added in portions, and after stirring for 1 h, the system was warmed to room temperature and stirred for 2 h. After removing the acetonitrile under

rotary evaporation, the residue was extracted with 100 mL of ethyl acetate; washed with water (2 × 30 mL), 1 M hydrochloric acid and saturated brine, dried over anhydrous sodium sulfate and concentrated over vacuum to give a brown crude product, which was purified by silica gel column chromatography eluting with petroleum ether/ethyl acetate 50:1 to give a pale yellow solid 6.501 g, yield 61.08%, m.p. 78.6–79.3 °C. <sup>1</sup>H NMR (CDCl<sub>3</sub>, 400 MHz) δ 3.84 (s, 3H, OCH<sub>3</sub>), 4.21 (s, 2H, CH<sub>2</sub>), 6.95 (d, *J* = 8.96 Hz, 2H, ArH), 7.18–7.38 (m, 5H, ArH), 7.54 (d, *J* = 8.96 Hz, 2H, ArH).

5-benzyl-*N*-(4-methoxyphenethyl)-4-(4-methoxyphenyl)thiazol-2-amine (**37**). Compound **43** (0.4 g, 1.45 mmol), 4-methoxyphenethylamine (0.6 g, 4.36 mmol), lithium hydroxide monohydrate (0.1 g, 2.61 mmol), 10 mL of DMF and 0.3 mL of water were added into a 50 mL pear-shaped flask. A catalytic amount of potassium iodide was then added. The mixture was refluxed for 8 h and monitored by TLC. To the reaction solution, 20 mL of 1 M hydrochloric acid was added, and the mixture was extracted with ethyl acetate (10 mL × 3). The organic phase was washed with 1 M hydrochloric acid, distilled water and saturated brine, dried over anhydrous sodium sulfate and concentrated over vacuum. The crude product was purified by column chromatography (petroleum ether/ethyl acetate = 1:15–1:5), and 0.31 g of a white solid was obtained. Yield 50%, m.p. 153–154 °C. <sup>1</sup>H NMR (DMSO-*d*<sub>6</sub>, 600 MHz) δ 2.79 (t, *J* = 7.4 Hz, 2H, CH<sub>2</sub>), 3.37 (td, *J*<sub>1</sub> = 7.3 Hz, *J*<sub>2</sub> = 5.7 Hz, 2H, CH<sub>2</sub>), 3.71 (s, 3H, OCH<sub>3</sub>), 3.76 (s, 3H, OCH<sub>3</sub>), 4.05 (s, 2H, ArCH<sub>2</sub>), 6.87–6.83 (m, 2H, ArH), 6.97–6.94 (m, 2H, ArH), 7.16 (d, *J* = 8.5 Hz, 2H, ArH), 7.19–7.22 (m, 3H, ArH), 7.31 (t, *J* = 7.5 Hz, 2H, ArH), 7.53–7.48 (m, 3H, ArH, NH); <sup>13</sup>C NMR (151 MHz, CDCl<sub>3</sub>) δ 167.35, 159.13, 158.30, 140.46, 130.46, 129.72, 129.69, 128.60, 128.18, 126.52, 114.04, 113.78, 55.26, 55.25, 47.65, 47.59, 34.55, 32.91.

5-(2-methoxybenzyl)-*N*-(4-methoxyphenyl)-4-phenylthiazol-2-amine (**38**). A quantity of 0.50 g of **41a** was dissolved in 5.0 mL of anhydrous ethanol and then (0.20 g, 1.57 mmol) of 1-(4-methoxyphenyl)thiourea was added. The mixture was refluxed for 3 h while monitoring the reaction by TLC. After completion, the mixture was cooled, and 25 mL of water was added. Then, aqueous ammonia was added to the reaction mixture to adjust the pH to approximately 8. The mixture was stirred for 2 h at room temperature and filtered, washed, dried and recrystallized with hot ethanol to obtain a beige solid (0.30 g, 51.1%), m.p. 138.1–139.2 °C. <sup>1</sup>H NMR (DMSO-*d*<sub>6</sub>, 600 MHz) δ 3.71 (s, 3H, CH<sub>3</sub>O), 3.77 (s, 3H, CH<sub>3</sub>O), 4.06 (s, 2H, ArCH<sub>2</sub>), 6.90 (t, *J* = 9.00 Hz, *J* = 2.40 Hz, 3H, ArH), 7.00 (d, *J* = 2.40 Hz, 1H, ArH), 7.11 (d, *J* = 7.20 Hz, 1H, ArH), 7.24 (t, *J* = 7.20 Hz, 1H, ArH), 7.35 (t, *J* = 7.20 Hz, 1H, ArH), 7.44 (t, *J* = 7.20 Hz, 2H, ArH), 7.53 (d, *J* = 9.00 Hz, 2H, ArH), 7.62 (d, *J* = 7.20 Hz, 2H, ArH), 9.81 (s, 1H, NH); <sup>13</sup>C NMR (151 MHz, CDCl<sub>3</sub>) δ 165.24, 156.97, 156.07, 133.90, 129.41, 128.63, 128.27, 128.26, 127.83, 127.53, 121.98, 121.95, 120.58, 114.48, 110.18, 55.48, 55.17, 27.15; ESI-MS *m/z* 403[M+H]<sup>+</sup>; IR (KBr, cm<sup>-1</sup>): 3172 (ν<sub>N-H</sub>), 3065, 2937, 2831, 1566, 1510, 1489, 1244, 1165, 1031, 818, 751, 689.

## 9. Biology

### 9.1. Cells and plasmids

HEK 293T cells were obtained from National Platform of Experimental Cell Resources for Sci-tech (Beijing, China). The pNL4-3.luc.R<sup>-</sup> plasmid was obtained from National Institute of Health AIDS Research and Reference Reagent Program. VSVG plasmid was kindly provided by Dr. Lijun Rong (University of Illinois at Chicago). Seven NNRTI-resistant mutations (K103N, Y181C, L100I/K103N, Y188L, K103N/P225H, K103N/G190A, K103N/V108I) were introduced into env-deficient HIV vector (pNL4-3.luc.R<sup>-</sup>) by overlapping extension PCR followed by subcloning back into pNL4-

3.luc.R<sup>E-</sup> using Apal and AgeI restriction sites, as previously reported [28].

### 9.2. Anti-HIV activity assay by pseudotyped viruses

VSVG plasmid and env-deficient HIV vector (pNL4-3.luc.R<sup>E-</sup> or pNL4-3.luc.R<sup>E-</sup><sub>RT-mutant</sub>) [29,30] were co-transfected into HEK 293T cells using the Ca<sub>3</sub>(PO<sub>4</sub>)<sub>2</sub> method [31]. Sixteen hours post-transfection, the cells were washed with PBS and fresh media was added. The supernatant, containing pseudotyped viruses, was collected 48 h post-transfection. The harvested virus solution was quantified using p24 concentrations, which were detected by ELISA (ZeptoMetrix, Cat.: 0801111) and diluted to 0.2 ng p24/mL.

HEK 293T cells were seeded on a 24-well plate one day prior to infection. The compounds were added into the target cells 15 min prior to infection. For each well, 0.5 mL of pseudoviruses were added (0.2 ng p24/mL). Forty-eight hours post-infection, infected cells were lysed in Cell Lysis Reagent (Promega). Luciferase activity of the cell lysate was measured by a Sirius luminometer (Berthold Detection System) according to the manufacturer's instructions.

### 9.3. Cytotoxicity

Cytotoxicity was tested by incubating the compound with the cells for 48 h under the same culture conditions as for anti-HIV activity assay, but no viruses were added. The cytotoxicity was measured using a Cell Proliferation Assay kit (Promega) according to the manufacturer's instructions.

## 10. Computational

### 10.1. Docking and 3D-QSAR

All of the calculations reported were performed on an HP Z800 workstation with Red Hat Enterprise Linux 5 system using the Tripos Sybyl-X 1.2 (Tripos Inc, St Louis, MO, USA) molecular modeling package. The parameters in the study were set to default values except for those specifically mentioned.

### Acknowledgments

This work was supported by the National Natural Basic Research Program of China (No. 8127356), the National Major Scientific and Technological Special Project for Infectious Diseases (No. 2013ZX10004601) and the Central Level, Scientific Research Institutes for Basic R & D Special Fund Business (2013ZD06).

### Appendix A. Supplementary data

Supplementary data associated with this article can be found in the online version, at <http://dx.doi.org/10.1016/j.ejmech.2014.07.072>. These data include MOL files and InChIKeys of the most important compounds described in this article.

### References

- [1] S.F. Barre, J. Chermann, F. Rey, M. Nugeyre, S. Chamaret, J. Gruest, C. Dauguet, B.C. Axler, B.F. Vezinet, C. Rouzioux, W. Rozenbaum, L. Montagnier, Isolation of a T-lymphotropic retrovirus from a patient for a risk of acquired immunodeficiency syndrome (AIDS), *Science* 220 (1983) 868–871.
- [2] R.C. Gallo, P.S. Sarin, E.P. Gelmann, G.M. Robert, E. Richardson, V.S. Kalyanaraman, D. Mann, G.D. Sidhu, R.E. Stahl, P.S. Zolla, J. Leibowitch, M. Popovic, Isolation of human T-cell leukemia virus in acquired immunodeficiency syndrome (AIDS), *Science* 220 (1983) 865–867.
- [3] UNAIDS Report on the Global AIDS Epidemic, 2013. <http://www.unaids.org/en/> (accessed 14.01.14).
- [4] S.H. Michaels, R. Clark, P. Kissinger, Declining morbidity and mortality among patients with advanced human immunodeficiency virus infection, *N. Engl. J. Med.* 339 (1998) 405–406.
- [5] P.K. Correll, M.G. Law, A.M. McDonald, D.A. Cooper, J.M. Kaldor, HIV disease progression in Australia in the time of combination antiretroviral therapies, *Med. J. Aust.* 169 (1998) 469–472.
- [6] S.C. Piscitelli, C. Flexner, J.R. Minor, M.A. Polis, H. Masur, Drug interactions in patients infected with human immunodeficiency virus, *Clin. Infect. Dis.* 23 (1996) 685–693.
- [7] M. Louie, M. Markowitz, Goals and milestones during treatment of HIV-1 infection with antiretroviral therapy: a pathogenesis-based perspective, *Antivir. Res.* 55 (2002) 15–25.
- [8] D. Boden, A. Hurley, L. Zhang, Y. Cao, Y. Guo, E. Jones, J. Tsay, J. Ip, C. Farthing, K. Limoli, N. Parkin, M. Markowitz, HIV-1 drug resistance in newly infected individuals, *JAMA J. Am. Med. Assoc.* 282 (1999) 1135–1141.
- [9] F.P. Pecora, I.R. McNicholl, Etravirine and rilpivirine: nonnucleoside reverse transcriptase inhibitors with activity against human immunodeficiency virus type 1 strains resistant to previous nonnucleoside agents, *Pharmacotherapy* 29 (2009) 281–294.
- [10] C.E. De, Anti-HIV drugs: 25 compounds approved within 25 years after the discovery of HIV, *Int. J. Antimicrob. Agents* 33 (2009) 307–320.
- [11] P.K. Cheung, B. Wynhoven, P.R. Harrigan, Which HIV-1 drug resistance mutations are common in clinical practice? *AIDS Rev.* 6 (2009) 107–116.
- [12] L. Tambuyzer, H. Azijn, L.T. Rinsky, J. Vingerhoets, P. Lecocq, G. Kraus, G. Picchio, M.P. de Bethune, Compilation and prevalence of mutations associated with resistance to non-nucleoside reverse transcriptase inhibitors, *Antivir. Ther.* 14 (2009) 103–109.
- [13] C. Bell, G.V. Matthews, M.R. Nelson, Non-nucleoside reverse transcriptase inhibitors; an overview, *Int. J. STD AIDS* 14 (2003) 71–77.
- [14] C.B. Guo, Y. Guo, Z.Z. Li, M.Y. Ba, Z.L. Xu, Y.L. Cao, R.C. He, Y. Yang, H. Zhou, Y.T. Li, Preparation of thiazole derivatives as anti-HIV agents, *Faming Zhuanli Shenqing* (2013). CN 103159695 A.
- [15] A.L. Hopkins, J. Ren, H. Tanaka, M. Baba, M. Okamoto, D.I. Stuart, D.K. Stammers, Design of MKC-442 (emivirine) analogues with improved activity against drug-resistant HIV mutants, *J. Med. Chem.* 42 (1999) 4500–4505.
- [16] J. Lindberg, S. Sigurdsson, S. Lowgren, H.O. Andersson, C. Sahlberg, R. Noreen, K. Fridborg, H. Zhang, T. Unge, Structural basis for the inhibitory efficacy of efavirenz (DMP-266), MSC194 and PNU142721 towards the HIV-1 RT K103N mutant, *Eur. J. Biochem.* 269 (2002) 1670–1677.
- [17] D.M. Himmel, K. Das, A.D. Clark Jr., S.H. Hughes, A. Benjahad, S. Oumouch, J. Guillemont, S. Coupa, A. Poncelet, I. Csoka, C. Meyer, K. Andries, C.H. Nguyen, D.S. Grierson, E. Arnold, Crystal structures for HIV-1 reverse transcriptase in complexes with three pyridinone derivatives: a new class of non-nucleoside inhibitors effective against a broad range of drug-resistant strains, *J. Med. Chem.* 48 (2005) 7582–7591.
- [18] M.L. Mitchell, J.C. Son, I.Y. Lee, C.K. Lee, H.S. Kim, H. Guo, J. Wang, J. Hayes, M. Wang, A. Paul, E.B. Lansdon, J.M. Chen, G. Eisenberg, R. Geleziunas, L. Xu, C.U. Kim, N1-heterocyclic pyrimidinediones as non-nucleoside inhibitors of HIV-1 reverse transcriptase, *Bioorg. Med. Chem. Lett.* 20 (2010) 1585–1588.
- [19] T.A. Kirschberg, M. Balakrishnan, W. Huang, R. Hluhanich, N. Kutty, A.C. Licican, D.J. McColl, N.H. Squires, E.B. Lansdon, Triazole derivatives as non-nucleoside inhibitors of HIV-1 reverse transcriptase-structure-activity relationships and crystallographic analysis, *Bioorg. Med. Chem. Lett.* 18 (2008) 1131–1134.
- [20] G. David, G. Helène, L.S. Jean, N. Michael, F.Z. Jean, M. Matthieu, Comparative evaluation of 3D virtual ligand screening methods: impact of the molecular alignment on enrichment, *J. Chem. Inf. Model.* 50 (2010) 992–1004.
- [21] K.S. Sree, M.M. Vijulatha, Receptor conformation docking and dock pose clustering as tool for CoMFA and CoMSIA anaKis a case study on HIV-1 protease inhibitors, *J. Mol. Model.* 18 (2012) 569–582.
- [22] C. Elena, B. Laura, F. Paola, 3,4,5-Trisubstituted-1,2,4-4H-triazoles as WT and Y188L mutant HIV-1 non-nucleoside reverse transcriptase inhibitors: docking-based CoMFA and CoMSIA analysis, *J. Mol. Model.* 17 (2011) 1537–1550.
- [23] H.M. Hao, Y. Li, Y.H. Wang, Y.L. Yan, S.W. Zhang, Combined 3D-QSAR, molecular docking, and molecular dynamics study on piperazinyl-glutamate-pyrimidines/pyrimidines as potent P2Y12 antagonists for inhibition of platelet aggregation, *J. Chem. Inf. Model.* 51 (2011) 2560–2572.
- [24] S. Wold, A. Ruhe, H. Wold, W. Dunn III, The collinearity problem in linear regression. The partial least squares (PLS) approach to generalized inverses, *SIAM J. Sci. Stat. Comput.* 5 (1984) 735–743.
- [25] W.J. Dunn, S. Wold, U. Edlund, S. Hellberg, J. Gasteiger, Multivariate structure-activity relationship between data from a battery of biological tests and an ensemble of structure descriptors: the PLS method, *Quant. Struct. Act. Relat.* 3 (1984) 31–137.
- [26] P. Geladi, Notes on the history and nature of partial least squares (PLS) modelling, *J. Chemom.* 2 (1988) 231–246.
- [27] R.D. Cramer III, J.D. Bunce, D.E. Patterson, Crossvalidation, bootstrapping and partial least squares compared with multiple regression in conventional QSAR studies, *Quant. Struct. Act. Relat.* 7 (1988) 18–25.

- [28] Y.L. Cao, S.X. Li, H. Chen, Y. Guo, Establishment of pharmacological evaluation system for non-nucleoside reverse transcriptase inhibitors resistant HIV-1, *Acta Pharm. Sin.* 44 (2009) 355–361.
- [29] J. He, S. Choe, R. Walker, P. Di Marzio, D.O. Morgan, N.R. Landau, Human immunodeficiency virus type 1 viral protein R (Vpr) arrests cells in the G2 phase of the cell cycle by inhibiting p34cdc2 activity, *J. Virol.* 69 (1995) 6705–6711.
- [30] R.I. Connor, B.K. Chen, S. Choe, N.R. Landau, Vpr is required for efficient replication of human immunodeficiency virus type-1 in mononuclear phagocytes, *Virology* 206 (1995) 935–944.
- [31] L. Rong, P.J. Bates, Analysis of the subgroup A avian sarcoma and leukosis virus receptor: the 40-residue, cysteine-rich, low-density lipoprotein receptor repeat motif of Tva is sufficient to mediate viral entry, *J. Virol.* 69 (1995) 4847–4853.